Neuroprotective Effect of Trehalose and Sodium Butyrate on Preformed Fibrillar Form of Alpha-Synuclein Induced Rat Model of Parkinson Disease

Introduction

Next to Alzheimer disease (AD), Parkinson disease (PD) is found to affect the worldwide population at a rate of 0.3% and 3% of those in the age group of 80 years[1]. Over 200 years ago, James Parkinson essay on the Shaking Palsy, became a driving force for digging deep into the underlying etiology of PD[2] still the only available therapeutic approach is based on symptomatic management. Slowness of movement, postural instability, rigidity, and tremor are some of the major motor features associated with PD.

Motor symptoms mainly occur due to dopamine (DA) loss in the substantia nigra pars compacta (SN) and its downstream impairment of basal ganglia activity[3]. Up to 80% of PD patients experience PD dementia (PDD) as the disease progresses[4],also cognitive abnormality is known to accompany before the motor symptoms onset or can build up as the disease progresses[5]. Neuropathologically, presence of lewy bodies (LBs) characterize both PD and PDD as devised by Friedrich Lewy in 1912[6]. And this led to the identification of alpha-synuclein (α-syn) as the primary component of LBs[7].

α-syn is a cytosolic protein and normally localized in the presynaptic terminals[8]. Once the neuron is affected, α-syn forms LBs in its soma[9]. α-syn inclusions initiates its formation over greater periods of time which might result in the LBs to affect only a subset of neurones[3]. However, neurones can also be affected by α-syn due to uptake of these inclusions by synaptically-connected neurons as evidenced by recent data from humans and model system leading to a pathological spread within the brain that correlates with disease progression. Progressive loss of motor coordination is the major symptom of PD attributable to dysregulation of basal ganglia activity which is largely due to the degeneration of DA neurons in the SN[9]. However, at later advanced stage of the disease, it has been found that α-synucleinopathy might spread to other brain regions including limbic areas, neocortical region, and brainstem[10].

Evidences suggest that preformed fibrillar form (PFF) of α-syn (hereby referred to as PFF α-syn) is the most toxic oligomeric form of α-syn and has been accepted as a well-established model for PD induction both *in vivo* and *in vitro*[11]. Normally, α-syn is degraded by the chaperone mediated form (CMA) of autophagy[12]. Autophagy, a self-degradative mechanism is responsible for disposing off damaged proteins maintaining the body decorum orchestrated by CMA, micro and macroautophagy. Aggregated/mutant forms of α-syn, for instance its PFF form inhibit CMA evoking in accumulation of damaged proteins and degenerating neurones with time. However, a study suggested that cell survival can be augmented through the vesicular protein sorting 34-beclin-1 complex, a secondary signalling pathway for autophagy initiation where beclin-1 overexpression causing reduced α-syn accumulation, decreases cell death and enhances lysosomal degradation[13] delineating the fact that enhancement in

autophagy clears out aggregated proteins and its tailored manipulation can help reduce PD pathology.

Trending research have confirmed trehalose (tre) role as an inducer of autophagy in various neurodegenerative models mainly attributed to its neuroprotective potential though microbiota-gut-brain signalling[14]. This hypothesis was further strengthened when it was established that autophagy induction in the mouse brain took place only after an oral intake of tre suggesting that the gastrointestinal (GI) system[15] plays a crucial role in the neuroprotective mechanism by tre. Moreover, Martano et al. reported that the mouse hippocampus and cortex evidenced presence of tre. Endogenous tre was present in astrocytes and neurons with its hydrolyzing enzyme, trehalase, present in neurons. Release of tre into the extracellular space[16] was facilitated by the astrocytes.

Treatment of tre to prion infected cells elevated microtubule-associated protein 1A/1B-light chain 3-phosphatidylethanolamine conjugate (LC3-II) levels increasing the basal levels of autophagy[17]. In the same study, de novo production of PrPSc aggregates were reduced along with its subcellular localizations alteration. An autophagic substrate, namely, p62/SQSTM1 was decreased by oral delivery of tre to Parkin-/-/TauVLW mice. Tre also prevented cell death induction due to polyubiquitinated proteins activated by a proteasome inhibitor, epoxomicin[18]. Tre altered epoxomicin-induced autophagic inhibition as evidenced by normal levels of LC3-II and p62/SQSTM1. In another study with an oral delivery of 1% tre (approximately, 1.9 - 2.3 g/kg) for 28 days could not reverse the 1-methyl-4-phenyl-1,2,3,6-tetrahydropyridine (MPTP) induced behavioural changes in C57Bl/6 mice, however the treatment could decrease the striatal DA, homovanillic acid (HVA) and 3,4-Dihydroxyphenylacetic acid (DOPAC)[19]. Sarkar *et. al*, demonstrated that, treatment with 2% of tre twice weekly for 5 weeks on MPTP induced PD on C57Bl/6 mice, decreased the MPTP induced loss in DA transporter and tyrosine hydroxylase (TH) in the caudate/putamen (CPu) and SnPC along with improved motor abnormalities[20]. In another study where rat injected with human A53T α-syn expressed virus vector undergone treatment with 0.5, 2 and 5% of tre for 6 weeks. The 0.5% tre treatment failed to improve neurochemical and behavioural deficits. However, 2 and 5% tre treatment could improve motor abnormalities, neurodegeneration, and α-syn aggregation in nigrostriatal system and elevated striatum LC3-II level[21].

Further, histone posttranslational modification causes autophagy induction as confirmed by a study conducted by Madeo, Kroemer, and coworkers, where, upon treatment with spermidine in aging yeast the cytoprotective autophagy activation occured majorly due to histone acetylation inhibition, specifically, Iki3 and Sas3, rendering global histone H3 hypoacetylation, with the repression of gene expression. Additionally, autophagy induction by numerous stimuli decreases the acetylation of histone H4 lysine 16 (H4K16ac). H4K16 deacetylation invokes a decreased level in the expression of autophagy-related genes, such as, ATG9A, MAP1LC3, GABARAPL2, VMP1, ULK1 and ULK3[22]. Inhibition of the autophagic H4K16 deacetylation increases autophagic flux instead of inhibiting autophagy proved form the outcomes of several experimental evidence which is consistent with genome-wide investigations. Similarly, di and trimethylation of histone H3 at lysine 4[23] and H4K20[24] controls the expression of major

autophagy related genes modulating transcriptional activation and repression. Lower histone acetylation levels are observed in AD and PD models[25], for instance, a histone deacetylase inhibitor (HDACi), valproic acid was found to be neuroprotective against rotenone induced PD[26]. Sodium butyrate (SB), a pan HDACi can elicit major neuroprotective potency against 6-hydroxydopamine induced PD in rats in lieu of its histone acetylation action and great blood brain barrier permeability as reported previously from our lab[27]. However, whether the neuroprotective efficacy of HDACis like valproic acid and SB is via autophagy modulation remains largely unknown.

Hence, in the current study, PFF α-syn was used to induce PD in wistar rats. 6 months after complete pathology formation, the rats were administered with an autophagy inducer, i.e., tre and a pan HDACi, SB. These drugs were administered singly and in combination to investigate its resultant effects on the behavioural outcome, expression of certain autophagy related genes, neuroinflammatory markers, pyknotic neuronal count and percentage positive cells for relevant proteins known to directly influence progression of PD pathology.

Material and methods

Animals

Male wistar rats (200-250g, 8-10week) were housed at central animal facility, BITS-Pilani, Pilani campus with standard laboratory conditions (temperature: 20-22°C, humidity: 65%) on a 12:12 hour light:dark cycle with food and water ad libidum. Institutional Animal Ethics Committee (IAEC) - BITS-Pilani, Pilani Campus, Rajasthan approved all experiments and sample collection (Approved protocol No: IAEC/RES/24/14).

Preparation of PFF α-syn

Briefly, recombinant human α-syn (1 mg) commercially available was obtained from Rpeptide and rapidly thawed and resuspended in distilled water to a final concentration of 1000 µl. The resuspended vial was then centrifuged at 100,000 g for 60 min in 4°C to pellet any aggregated material. Following which, the tube was placed in a thermomixer which is maintained at 37°C (this avoids condensation, which will affect the concentration of fibril). The tube was then shaken for 7 days at 1000 rotation per minute (rpm) along-with probe sonication for 30 sec (0.5 sec pulse on and off). The solution in the tube appeared turbid after 7th day. The final solution after shaking for 7 days was divided in 20µl aliquots into sterile microcentrifuge tubes and stored at −80°C for further use[51]. Confirmation of the formation of PFF was done by coomassie staining.

Sedimentation assay for PFF α-syn

20µl of PFFs was pipetted into a tube which was centrifuged at 100,000g for 60min at room temperature. 20µl of supernatant was removed and transferred to a new tube to which 20µl of 2× Laemmli buffer was added. 20µl of PBS was used to suspend the pellet and centrifuged again at 100,000g for 30min. The supernatant was removed. To this fraction the pellet was suspended in 20µl of PBS, and 20µl of 2× Laemmli buffer was added. 15µl of the supernatant from the first step and pellet from the last step was added onto a 4–20% (wt/vol) acrylamide

gel with a 15-well comb to perform Coomassie staining and destaining. Approximately equivalent amounts of α-syn should run above the 15-kDa marker in the supernatant and pellet as is observed in the Supplementary figure 2.

Stereotaxic injection of PFF α-syn

Eight-week old wistar rats were deeply anesthetized with 4% chloral hydrate solution. PBS in the sham control group and PFF α-syn (pelleted form) in the disease group (5 μg) were unilaterally injected into striatum at two points (2.5 μl per hemisphere at 0.5 μl/ min) using the coordinates: anteroposterior (AP) = +0.2 mm, mediolateral (ML) = +2.0 mm, dorsoventral (DV) = +2.8 mm and AP= +1.0 mm, ML= +1.5 mm, DV= -2.8 mm from bregma[51]. After the injection, the needle was kept as such for next 5 min for complete absorption of the solution. PFF α-syn have been proven to inflict PD pathology post 6 months after its seeding[51]. Treatment with tre and SB was initiated thereafter.

Experimental protocol

Each group comprised of 8 animals with 6 groups as described in table 1. 28 days treatment with tre and SB were initiated by freshly preparing everyday by dissolving in normal saline followed by vortexing before administration. Dose for SB was selected based on study conducted previously in our lab [27] whereas dose of tre for neuroprotection was selected based on available literature[19–21].

S. No.	Group	Treatment
1	Normal control	The animals without any infusion into the striatum.
2	Sham control	Animals were infused with PBS in the striatum.
3	PFF α-syn	Animals were infused with PFF α-syn intrastriatally.
4	Tre, 4 g/kg	PFF α-syn animals were administered with tre 4 g/kg, orally.
5	SB, 300 mg/kg	PFF α-syn animals were administered with SB 300 mg/kg, orally.
6	Tre and SB	PFF α-syn animals were administered with tre (2 g/kg) and SB (150 mg/kg), orally.

Table 1: Experimental groups division with their respective treatment.

Behavioural parameters assessment

Rotarod test: The rotarod test is generally used to access the motor performance of the rodents and is a well-accepted model for assessing the extent of PD neuronal degeneration. As the first symptom of PD is motor imbalance, hence rotarod test is always the first choice of any researcher for analysing PD pathology. Briefly, each animal was allowed to move on a rotating rod at an initial rpm of 5 which was progressively increased to 15 rpm. The ability to hold on to the rotating rod even at high speed was considered as the normal motor functionality of the rodent. The time to fall (in seconds) was recorded for each animal[52].

Open field test: This test is mainly used to access the locomotor activity, anxiety, and willingness of rodents to explore novel environments. Originally developed by Calvin S. Hall,

the principle of open field test is to rule out the anxious and exploratory behaviour of the rodents. During PD, immobility is the first symptom that is normally seen in most of the cases along with the occurrence of anxiety eventually. Hence, decreased mobility with increased anxiety was considered as a parameter to access the severity of PD progression [53]. Briefly, the apparatus consisted of an open field with a wall consisting of grid and square crossings where the rodents were placed in the arena for a period of 15 mins and total distance travelled by each animal was recorded [54].

NBW test: The rationale of this test is to assess the time traversed by the animal to move across a thin beam from one end to other end, consisting of a safe platform. Number of paw slips during the process was also recorded[55]. The apparatus comprises of a thin beam held up 1m above the ground. The black coloured platform is provided with a cushion and the narrow beam placed freely in this cushion. 60s and maximum 5-foot slips was allotted to each animal and the time taken to move across the beam along with the total number of foot slips were recorded manually[52].

Novel object location and recognition test: Cognitive dysfunction is one of the major non-motor symptoms occurring during late or early PD. The NOR and NOL test is used to rule out the cognitive anomaly of the rodent. The test comprises of four steps i.e. habituation, training, novel object, and novel location recognition test. Briefly, in the habituation step, the rat is freely allowed to explore in open field area for a period of 15 min in the absence of objects on the first day. The following day i.e. in the training phase, the rats were presented with two similar looking objects in the same open field and allowed to explore for a period of 5 min. Post 24 h, the animal was presented with one similar object and a novel object[56], following which, the animal was again placed in the same arena with a similar object along with a novel object and a novel location. The duration of the animal to explore the novel object and the novel location was recorded for a period of 5 min[57] and was considered as a measure of extent of cognitive damage.

Assessment of biochemical parameters

Hippocampus/SN homogenate preparation

Decapitation was employed to sacrifice the animals following which the desired region of the brain, i.e. hippocampus/SN were isolated and washed with ice-cold sodium chloride (0.9% w/v), afterwards these parts were homogenized with ice cold PBS (0.1M, pH 7.4) with 10 times (w/v) volume of the weight of the tissue. The homogenate was centrifuged at 12,000 g for 15min at 4°C and the supernatant obtained was divided into aliquots and utilized for biochemical estimations.

Protein estimation

Brain hippocampus/SN protein level was assessed by the Lowry method using bovine serum albumin (1 mg/ml) as a standard[58].

Estimation of pro-inflammatory cytokine TNF-α, IL-1, and IL-6 level

Neuroinflammatory markers like TNF-α, IL-1 and IL-6 in the hippocampal and the nigral homogenate were estimated using ELISA kit as per directions from manufacturer. The values were represented as picogram per milligram of protein.

Estimation of CRP level

CRP level was measured in the striatum homogenate as per the specifications given by the procured ELISA kit.

Estimation of BDNF level

BDNF level was assessed in SN homogenates with commercially available ELISA kit as per the instructions from manufacturer.

Estimation of DA level

DA level was estimated in SN as well as the striatum homogenates by using a commercially available ELISA kit as per the instructions from manufacturer.

Estimation of global histone H3 acetylation level

Global Histone H3 acetylation EpiQuik™ Assay Kit was used to determine Global Histone H3 Acetylation level as per instruction from manufacturer.

Ribonucleic acid (RNA) isolation and qPCR

TRIzol™ Reagent (Invitrogen™, 15596018) was used to extract the total RNA from the brain homogenate. Synthesis of complementary deoxyribonucleic acid (cDNA) was carried out using RevertAid Reverse Transcriptase (Thermo Fisher, EP0441) along with Random hexamer (Thermo Fisher, SO142).

Real-time quantitative polymerase chain reaction (qPCR)

The CFX Connect Optics Module (Bio-Rad) was used for qPCR assays. 2X Maxima SYBR Green/ROX qPCR Master Mix (Thermo Fisher, K0221) with specific primers was used for amplification according to manufacturer's instructions (Table 2). The conditions for PCR were 95°C (10 min), 40 cycles of 95°C (15s), 60°C (30s) and 72°C for (30s). The $2^{-\Delta\Delta CT}$ method was employed for calculating the relative mRNA expression level[59].

Gene	Forward Primer	Reverse Primer
Beclin 1	AGCTGCCGTTATACTGTTCTG	ACTGCCTCCTGTGTCTTCAATCTT
LC3-II	GATGTCCGACTTATTCGAGAGC	TTGAGCTGTAAGCGCCTTCTA
LAMP-2	AGCCCCAAACAGCTCAACTT	TATGATGGCGCTTGAGACCA
TH	AGGGCTAAATACGGCTGCTC	CAGCTGCTTCACAGACCCAT
DAT	GCTGCGTCACTGGCTGTTGC	CTGTCCCCGCTGTTGTGAGGT
α-syn	GAGGGAGTCGTTCATGGAGT	CATTTGTCACTTGCTCTTTGG

MAP-2	CGGAAAACCACAGCAGCAAG	ACTTTGGAGGAGTGCGGATG
GAPDH	AGGTCGGTGTGAACGGATTT	TTCCCGTTGATGACCAGCTT

Table 2: Primer sequences for *in-vivo* experiments.

Western blot analysis

Total protein was extracted from the SN by using RIPA buffer that contained phosphatase and protease inhibitors. Equal amount of lysates were separated by electrophoresis on an SDS-PAGE gel and transferred onto nitrocellulose membrane. The blot was probed overnight with primary antibodies, SQSTM1 antibody (Thermo Fisher Scientific), anti-LC3 (Sigma-Aldrich) and anti-β-actin (Sigma-Aldrich) at 4°C. Corresponding HRP-labeled secondary antibody (goat anti-rabbit IgG antibody, Sigma-Aldrich) was used and the signals were visualized using an ECL kit (Thermo Fisher Scientific).

Assessment of histopathological changes

10% v/v formalin was used as a fixing immersion median after rapid removal of the brains. Paraffin wax was utilized for embedding the brain by cutting into 5μm thick sections and then rehydrated with standard steps. Haematoxylin & eosin stain (H & E) were then used to stain these sections along with dehydration combined with clearing and coverslipping. SN region was analysed with Optika TCB5 microscope (Optika Research Microscope, Italy) at objective magnification of 10X and 40X. Photomicrographs of H&E stained sections were imported to Image J software (NIH-sponsored public domain image analysis software) and analysed. Neurons with degenerating characters were calculated using the Image J cell counter and represented as the percentage of degenerating neurons.

Immunofluorescence analysis of brain tissue

Briefly, the rats were overdosed with pentobarbital (50 mg/kg) to anesthetize and perfused with heparinized saline and then 10% paraformaldehyde (PFA) using Gilson Minipuls 2. After isolation, the brain was stored in PFA overnight and transferred to 20% sucrose solution for cryoprotection thereafter. After 3 days, the brain tissues, specifically the SN region were sectioned into 50 μm thick sections with a Leica sliding microtome, collected in PBS and transferred in anti-freezing solution until further processed for immunofluorecence. The sections were then washed in 0.1M PBS to remove the freezing solution and then incubated with blocking buffer, followed by incubation with necessary primary antibodies at 4˚C. PBS was then used to wash the sections followed by incubation with a secondary antibody and staining the nuclei with DAPI. Finally, the sections were visualized under an Invitrogen EVOS M7000 imaging system.

Statistical Analysis

Results expressed as mean ± SD. Statistical graph pad prism software (version 6.01 and 8.4.3) were used to analyse the behavioural and biochemical parameters by one-way analysis of variance (ANOVA) followed by Tukey's post hoc test. Histological and immunofluorescence photomicrographs were measured using ImageJ software.

Results

I. Effect of tre and SB on rotarod test

Rotarod test has been widely accepted as a model for assessment of motor abnormality disorder. During the test, the animals injected with PFF α-syn had a decreased fall of time from the revolving rod in comparison with sham control animals. Group treated with tre alone does not have any significant difference when compared with the disease group whereas the group treated with SB alone faintly improved the condition ($^{***}P\leq0.001$) but the group treated with a combination of tre and SB had a significant rise in the fall of time ($^{****}P\leq0.0001$) from the revolving rod on comparison with the disease group. Moreover, in the combination group a significant increase in the fall of time was observed when compared with tre ($^{****}P\leq0.0001$), but not with SB (figure 1).

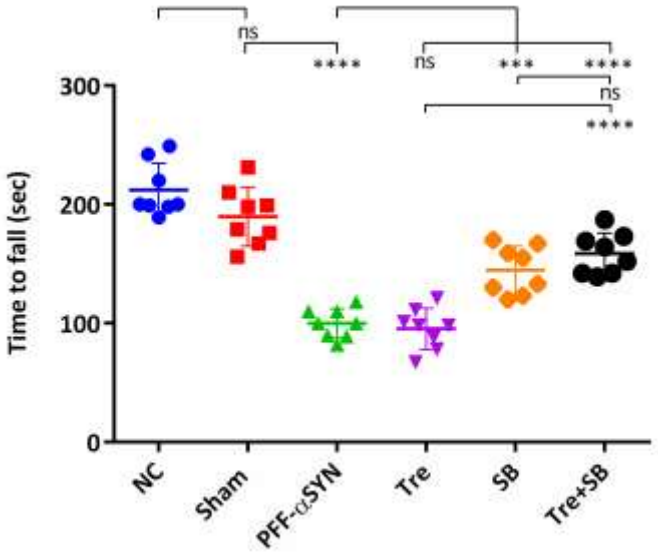

Fig. 1: Effect of tre and SB on rotarod test: Values represents Mean ± SD, $^{****}P\leq0.0001$ (Sham vs PFF α-syn); ns (PFF α-syn vs tre); $^{***}P\leq0.001$ (PFF α-syn vs SB); $^{****}P\leq0.0001$ (PFF α-syn vs tre+SB); $^{****}P\leq0.0001$ (tre+SB vs tre); ns (tre+SB vs SB), F (5,42) = 46.54, P<0.0001, ns: non-significant, NC: normal control.

II. Effect of tre and SB on open field test

Open field test is mainly used to access any abnormality related to locomotor activity and speed of locomotion of the animals that might result in immobility. Due to its ease of use and easily distinguishable features, this test provides an unbiased conclusion of the degree of severity of PD. During the test, the total distance travelled by each animal was calculated where it was observed that the distance travelled was reduced in case of diseased animals ($^{****}P\leq0.0001$) upon comparison with the sham control group. The group treated with tre alone had a non-significant difference in distance travelled when compared to the disease group. However, statistically significant result was being observed in the group administered with SB alone ($^{*}P\leq0.05$) and the combination treated group, i.e., tre and SB ($^{****}P\leq0.0001$). Further, in the combination group the distance travelled was significantly increased when compared with tre

(****P≤0.0001) but not with SB, suggesting that the combination group might possess an increased therapeutic potency as compared to either of the drugs alone (figure 2).

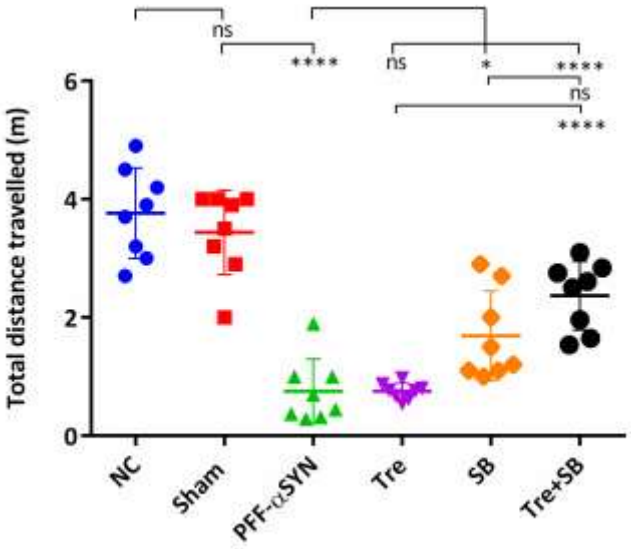

Fig. 2: Effect of tre and SB on total distance travelled: Values represents Mean ± SD, ****P≤0.0001, (Sham vs PFF α-syn); ns (PFF α-syn vs tre); *P≤0.05 (PFF α-syn vs SB); ****P≤0.0001 (PFF α-syn vs tre+SB); ****P≤0.0001 (tre+SB vs tre); ns (tre+SB vs SB), F (5,42) = 34.85, P<0.0001, ns: non-significant, NC: normal control.

III. Effect of tre and SB on NBW test

NBW test is widely used to rule out gait abnormalities in a PD induced animal. During the test, the analysis is done by measuring the duration of the animal to reach the platform. Here, the diseased group took a longer time to reach the home cage (****P≤0.0001) as compared to the sham control group and the treated groups. The combination group had a statistically significant decrease (****P≤0.0001) in the amount of time taken to reach the target platform and similar is the case observed with the group treated with SB alone (****P≤0.0001) when compared with the disease group. However, the group treated with tre alone had no significant difference. Further, the combination group demonstrated a significant decrease in the duration of animal to reach the platform when compared with tre (****P≤0.0001) but not with SB (figure 3A). Additionally, the number of foot paw slips was analysed in this test and the slips were decreased in the treated group with SB alone (**P≤0.01) with a more pronounced effect observed in the combination group (****P≤0.0001) in comparison with the disease group and no significance observed for the tre group. Moreover, when the combination group compared with tre a significant decrease in paw slip was observed (****P≤0.0001) but not with SB treatment (figure 3B).

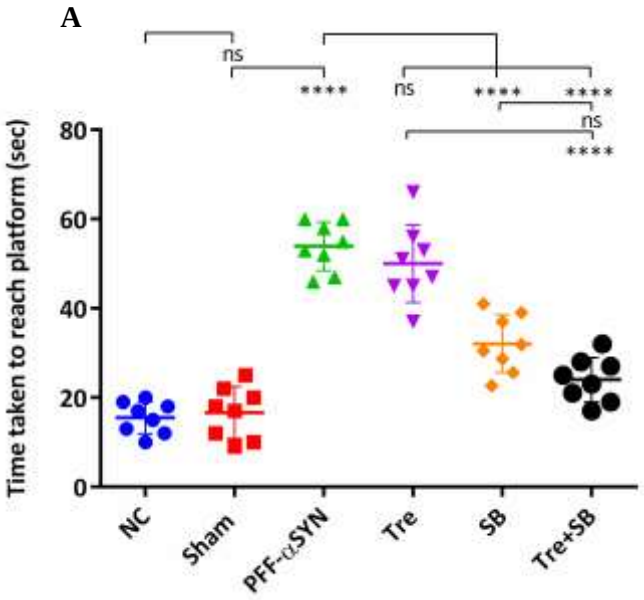

Fig. 3A: Effect of tre and SB on time taken to reach the platform: Values represents Mean ± SD, ****P≤0.0001, (Sham vs PFF α-syn); ns (PFF α-syn vs tre), ****P≤0.0001 (PFF α-syn vs SB); ****P≤0.0001 (PFF α-syn vs tre+SB); ****P≤0.0001 (tre+SB vs tre); ns (tre+SB vs SB), F (5,42) = 60.31, P<0.0001, ns: non-significant, NC: normal control.

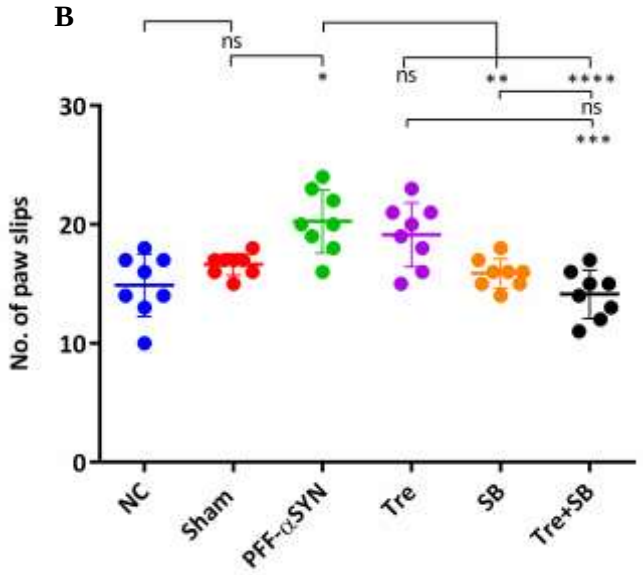

Fig. 3B: Effect of tre and SB on no of foot paw slips: Values represents Mean ± SD, *P≤0.05 (Sham vs PFF α-syn); ns (PFF α-syn vs tre); **P≤0.01 (PFF α-syn vs SB); ****P≤0.0001 (PFF α-syn vs tre+SB); ***P≤0.001 (tre+SB vs tre); ns (tre+SB vs SB), F (5,42) = 10.02, P < 0.0001, ns: non-significant, NC: normal control.

IV. Effect of tre and SB on NOR and NOL test

NOR and NOL test is a widely known model to govern any cognitive anomaly present in rodents. Studies suggest that PD is associated with cognitive disturbances either at a later

advanced stage of the disease or as a pre warning sign before the occurrence of its pathology. Having said that, it is extremely necessary to perform a memory recognition task to accurately speculate the progression of PD pathology and its amelioration by the treated groups. The task consisted of four stages:

- **Stage 1:** The animals could freely roam in an open field and the results were found to be statistically insignificant for all the groups at this stage shown in figure 4a.

- **Stage 2:** The animals were trained in the presence of two similar objects as shown in figure 4b, where the sham control group had an increased tendency to explore upon comparison to disease group ($^{***}P \leq 0.001$) but all the treated groups had a statistically insignificant result.

- **Stage 3:** The animals were provided with an acquainted or familiar and an unacquainted or novel object as shown in figure 4c, where a significant object recognition quality for SB ($^{**}P \leq 0.01$) and in combination group i.e., tre and SB ($^{****}P \leq 0.0001$) were observed upon comparison with the disease group. Moreover, when the combination group demonstrated a significant increase in time traversed when compared with tre and SB treatments in alone ($^{****}P \leq 0.0001$ for both tre+SB vs tre and tre+SB vs SB). The discrimination index demonstrates a significant increase in tre, SB and in combination group when compared with disease group ($^{****}P \leq 0.0001$, for all group vs PFF α-syn).

- **Stage 4:** The animals were presented with one familiar object but with a new location for one of the objects as shown in figure 4d. It was observed that the combination group had a potent effect in location test when compared to the disease group ($^{****}P \leq 0.0001$). Whereas tre and SB treated group had a little significant difference when compared with disease group ($^{*}P \leq 0.05$ and $^{**}P \leq 0.01$ respectively). However, significant change was observed in the combination group when compared with tre and SB ($^{***}P \leq 0.001$ and $^{**}P \leq 0.01$ respectively). The discrimination index indicates a marked significant difference in tre, SB and in combination ($^{****}P \leq 0.0001$) group when compared with disease group. In addition, the combination group had a significant increase in discrimination index when compared with tre ($^{*}P \leq 0.05$).

  The movement of each animal was tracked and recorded using ANYMAZE software (Stoelting, USA) (figures 4a-4d). The total distance traversed by the animal and the discrimination index were calculated using below formula and quantified using graph pad prism software.

$$\%\ \text{Discrimination index} = \frac{(\text{time with novel object or location} - \text{time with familiar object or location})}{(\text{time with novel object or location} + \text{time with familiar object or location})}$$

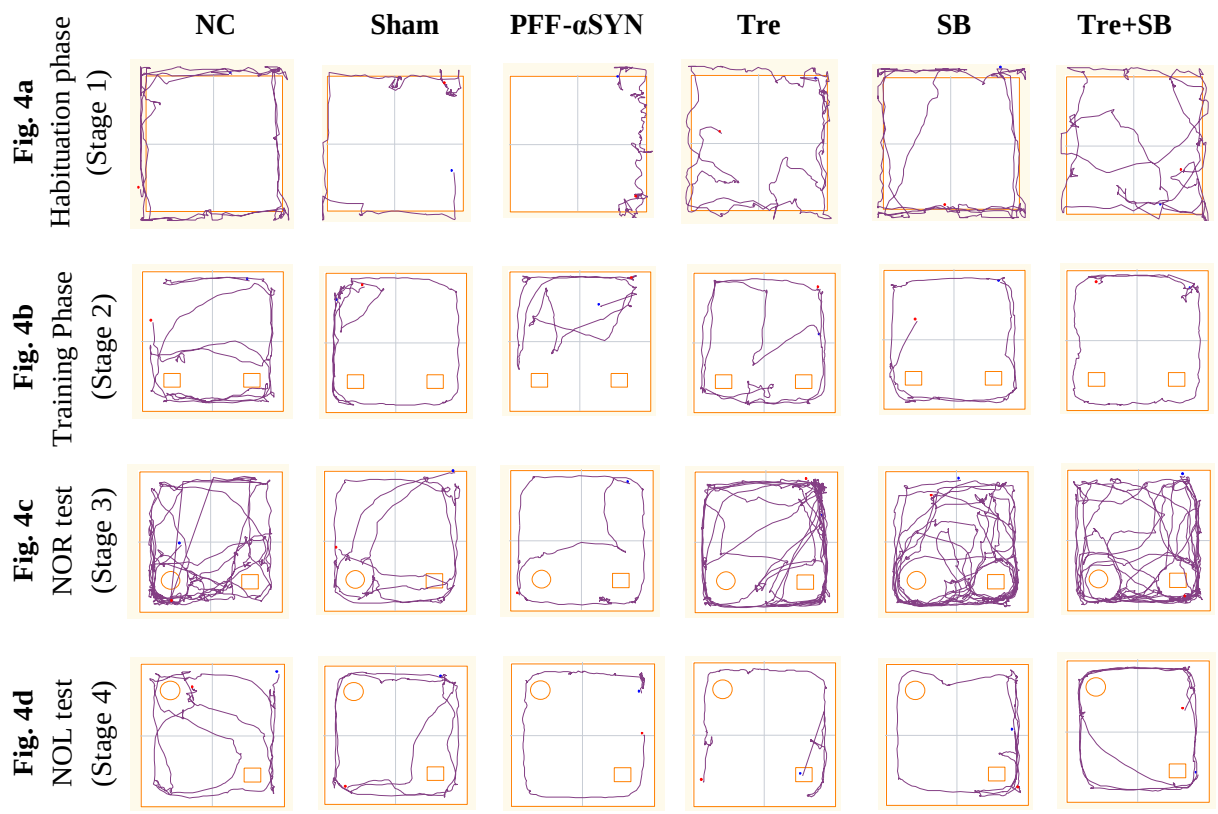

Fig. 4a-4d: Track plot of animals traversed during habituation phase, training phase, NOR and NOL test.

V. Effect of tre and SB on TNF-α, IL-1, and IL-6 level

PD pathology is accompanied by extensive loss of DA neurones in the SN. Evidence strongly point towards the extreme sensitivity of DA neurones for TNF-α, IL-1 and IL-6. The levels of these inflammatory markers drastically increase in case of experimental PD models. In the present study, we estimated the levels of TNF-α, IL-1 and IL-6 using commercially available ELISA kit and found that its levels increased in PD induced animals on comparison with the sham group ($^{****}P\leq0.0001$) but the levels were found to decrease in case of the combination treated group ($^{****}P\leq0.0001$) when compared with the disease group. However, little significant difference being observed for the group treated with SB alone ($^{*}P\leq0.05$, for TNF-α; $^{***}P\leq0.001$, for IL-1 and IL-6) and no statistical significance being observed for the group treated with tre alone in hippocampal region. Further, combination group compared with treatments in alone, a significant decrease was observed with tre ($^{**}P\leq0.01$) but not with SB for TNF-α, similarly for IL-1, tre+SB vs tre shows a significant change of $^{*}P\leq0.05$. The level of IL-6 was found significantly diminished in the combination group when compared with treatments in alone, $^{****}P\leq0.001$ for tre+SB vs tre and $^{**}P\leq0.01$ for tre+SB vs SB which suggest a better suppression of neuroinflammation in the combination group when compared with single administration (figure 5a-5c). To better arrive at a conclusion we have also performed estimation of these cytokines for the nigra region where we have observed similar decreasing trend in the

neuroinflamatory markers same as that in the hippocampal region on treatment with tre, SB alone and in combination (figure 6a-6c).

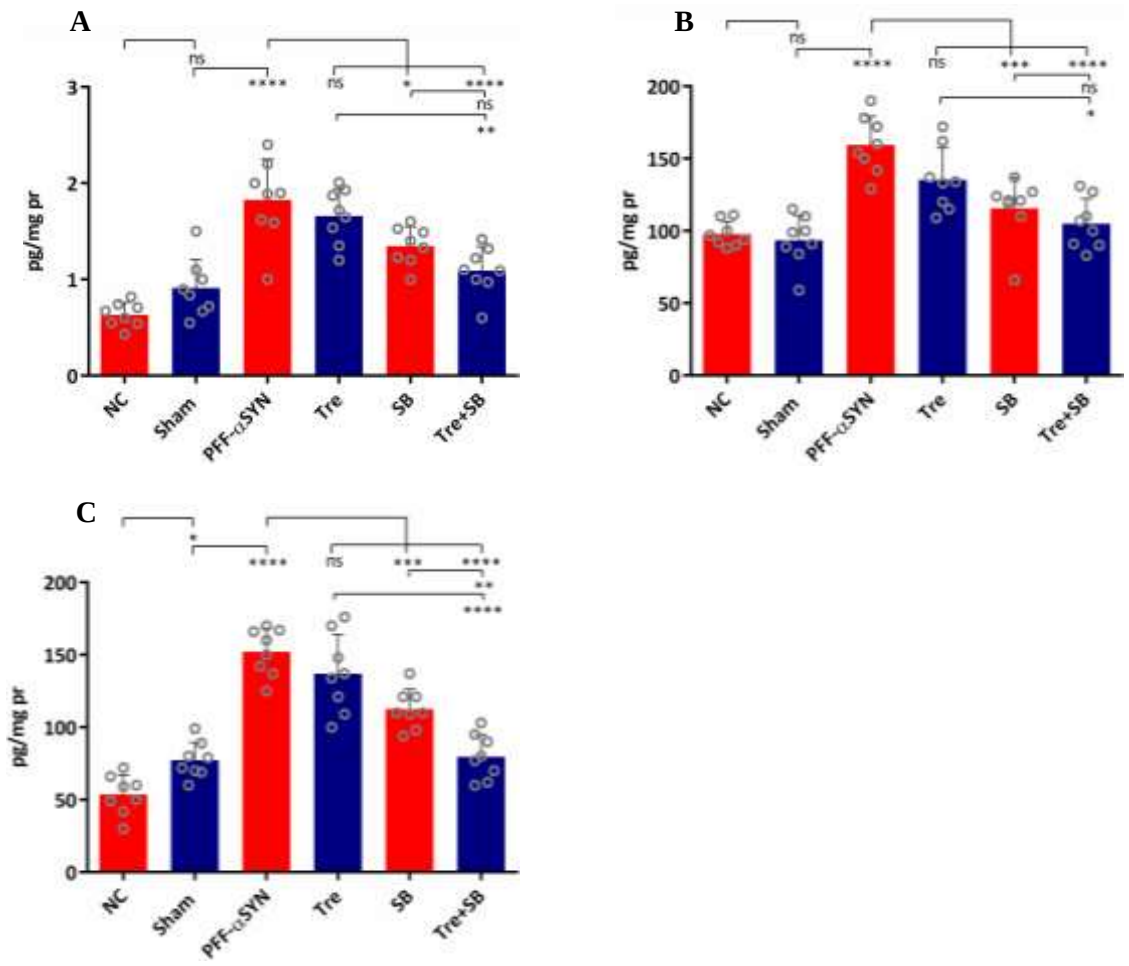

Fig. 5: (A) Effect of tre and SB on TNF-α levels in hippocampal region: Values represents Mean ± SD, ****P≤0.0001 (Sham vs PFF α-syn); ns (PFF α-syn vs tre); *P≤0.05 (PFF α-syn vs SB); ****P≤0.0001 (PFF α-syn vs tre+SB); **P≤0.01 (tre+SB vs tre); ns (tre+SB vs SB), F (5,42) = 20.93, P<0.0001; **(B)** Effect of tre and SB on IL-1 levels: Values represents Mean ± SD, ****P≤0.0001 (Sham vs PFF α-syn); ns (PFF α-syn vs tre); ***P≤0.001 (PFF α-syn vs SB); ****P≤0.001 (PFF α-syn vs tre+SB); *P≤0.05 (tre+SB vs tre); ns (tre+SB vs SB), F (5,42) = 15.18, P<0.0001; **(C)** Effect of tre and SB on IL-6 levels: Values represent Mean ± SD, ****P≤0.0001, (Sham vs PFF α-syn); ns (PFF α-syn vs tre); ***P≤0.001 (PFF α-syn vs SB); ****P≤0.001 (PFF α-syn vs tre +SB); ****P≤0.0001 (tre+SB vs tre); **P≤0.01 (tre+SB vs SB), F (5,42) = 39.65, P<0.0001, ns: non-significant, NC: normal control.

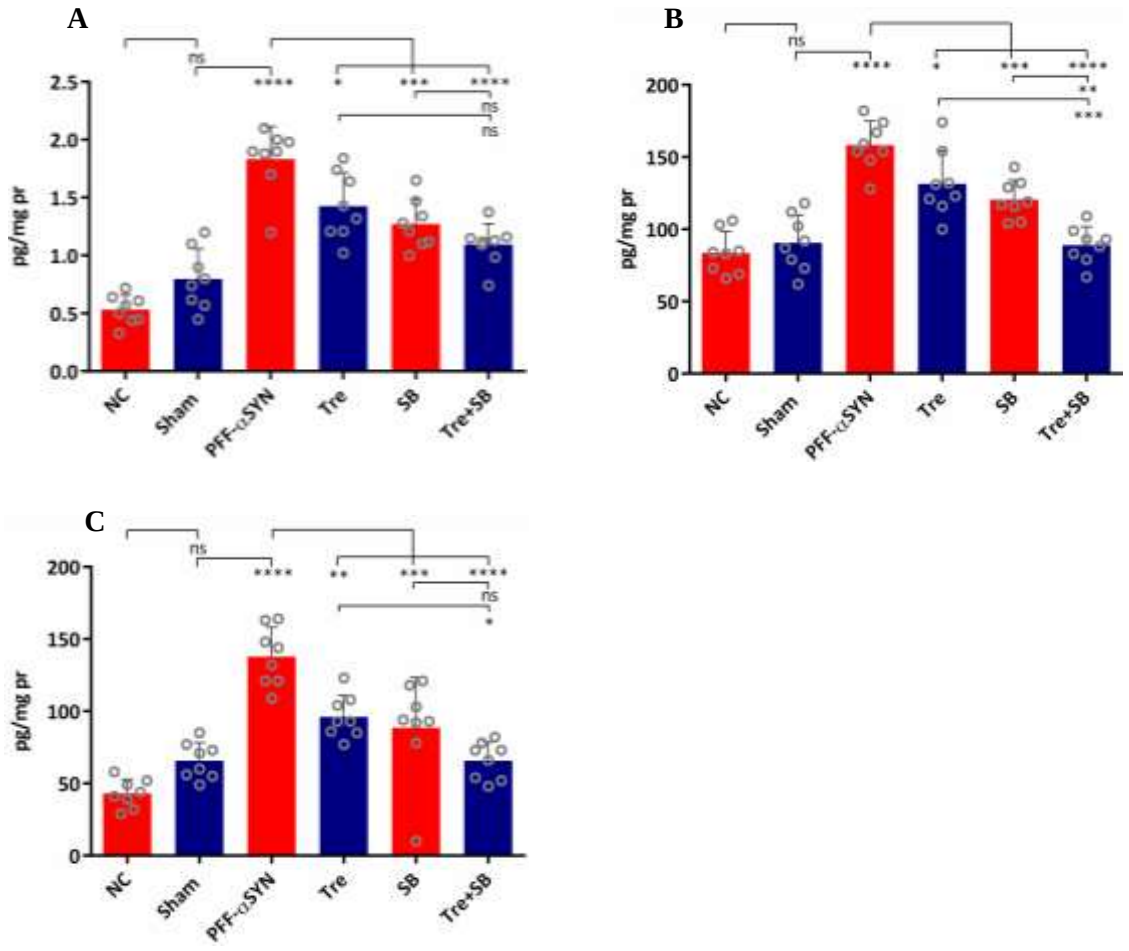

Fig. 6: (A) Effect of tre and SB on TNF-α levels in nigra region: Values represents Mean ± SD, ****P≤0.0001 (Sham vs PFF α-syn); *P≤0.05 (PFF α-syn vs tre); ***P≤0.001 (PFF α-syn vs SB); ****P≤0.0001 (PFF α-syn vs tre+SB); ns (tre+SB vs tre); ns (tre+SB vs SB), F (5,42) = 31.69, P<0.0001; **(B)** Effect of tre and SB on IL-1 levels: Values represents Mean ± SD, ****P≤0.0001 (Sham vs PFF α-syn); *P≤0.05 (PFF α-syn vs tre); ***P≤0.001 (PFF α-syn vs SB); ****P≤0.0001 (PFF α-syn vs tre+SB); ***P≤0.001 (tre+SB vs tre); **P≤0.01 (tre+SB vs SB), F (5,42) = 24.12, P<0.0001; **(C)** Effect of tre and SB on IL-6 levels: Values represent Mean ± SD, ****P≤0.0001, (Sham vs PFF α-syn); **P≤0.01 (PFF α-syn vs tre); ***P≤0.001 (PFF α-syn vs SB); ****P≤0.0001 (PFF α-syn vs tre+SB); *P≤0.05 (tre+SB vs tre); ns (tre+SB vs SB), F (5,42) = 22.89, P<0.0001, ns: non-significant, NC: normal control.

VI. Effect of tre and SB on level of CRP

CRP is an acute-phase protein and considered an intensive biomarker of systemic inflammation. In neurodegenerative disorders like PD and AD, an increase in the levels of CRP is indicative of the severity of neurodegenerative pathology. Hence in the current study, we analysed the expression of CRP and found that PFF α-syn markedly elevated CRP level (****P≤0.0001) on comparison with sham group indicating the progression of inflammatory process in that group. However, the combination group (****P≤0.0001) and the group treated with SB alone (***P≤0.001) markedly reduced the CRP levels compared to the disease group.

For the tre treatment in alone, although a decreased level of CRP was observed, but it was not significant when compared with disease group. Further, upon comparing the combination group with tre and SB treatments in alone, significant decrease in CRP was observed with tre (****P≤0.0001) and SB (**P≤0.01) (figure 7).

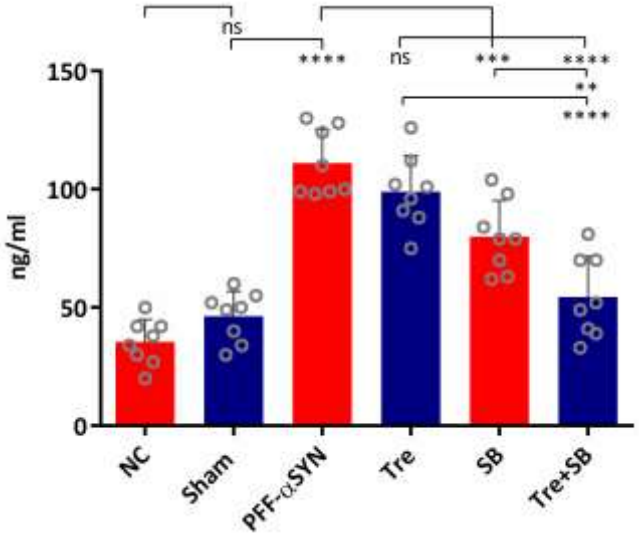

Fig. 7: Effect of tre and SB on CRP levels: Values represents Mean ± SD, ****P≤0.0001 (Sham vs PFF α-syn); ns (PFF α-syn vs tre); ***P≤0.001 (PFF α-syn vs SB); ****P≤0.0001 (PFF α-syn vs tre+SB); ****P≤0.0001 (tre+SB vs tre); **P≤0.01 (tre+SB vs SB), F (5,42) = 37.66, P<0.0001, ns: non-significant, NC: normal control.

VII. Effect of tre and SB on level of BDNF

The main function of BDNF lies in its ability to influence neuronal development, neurogenesis, synaptogenesis, synaptic plasticity, and cell differentiation. Normally, BDNF is known to regenerate DA neurones increasing its survival and ultimately improving the motor performance which is reversed during PD[28]. In this study, we conducted ELISA assay for BDNF to assess whether BDNF levels can be restored on treatment with tre and SB. We observed that PFF α-syn induced animals had a decreased expression of BDNF (****P≤0.001) on comparison with sham control which was efficiently restored in the groups treated with the SB alone (***P≤0.001) and in combination of tre and SB (****P≤0.0001). No statistical difference was observed for the group treated with tre alone. Further, the combination group demonstrated significant increase in expression level in contrast to that of the tre (****P≤0.0001) and SB (***P≤0.001) alone treatment (Figure 8).

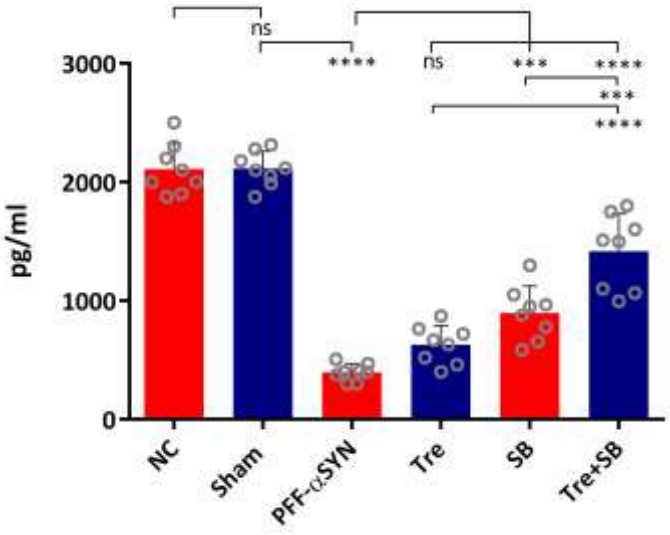

Fig 8: Effect of tre and SB on BDNF levels: Values represents Mean ± SD, ****P≤0.0001 (Sham vs PFF α-syn); ns (PFF α-syn vs tre); ***P≤0.001 (PFF α-syn vs SB); ****P≤0.0001 (PFF α-syn vs tre+SB); ****P≤0.0001 (tre+SB vs tre); ***P≤0.001 (tre+SB vs SB), F (5,42) = 105.8, P<0.0001, ns: non-significant, NC: normal control.

VIII. Effect of tre and SB on levels of DA

The predominant pathology arising during PD is loss of DA neurones exclusively in the SN region of the brain degenerating that region over time affecting movement control in an individual. Here, we went on to further check the levels of DA before and after treatment with tre and SB and found that DA levels were considerably reduced in the PFF α-syn group (****P≤0.0001) in contrast to that of the sham group and significantly restored on administration with SB alone (***P≤0.001) and in combination of tre and SB group (****P≤0.0001). The animal group administered with tre alone was found to be statistically not significant. However, when combination group compared with treatments in alone, a marked significant increase in DA level was observed as ****P≤0.0001 for tre+SB vs tre and **P≤0.01 tre+SB vs SB (figure 9A). Results from the DA estimation for the striatum region revealed similar results as that of SN region when compared to the disease group with a significant increase observed for the tre group (*P≤0.05). The combination group when compared with treatments in alone also demonstrated significant increase in DA as ***P≤0.001 for tre+SB vs tre and *P≤0.05 tre+SB vs SB (figure 9B).

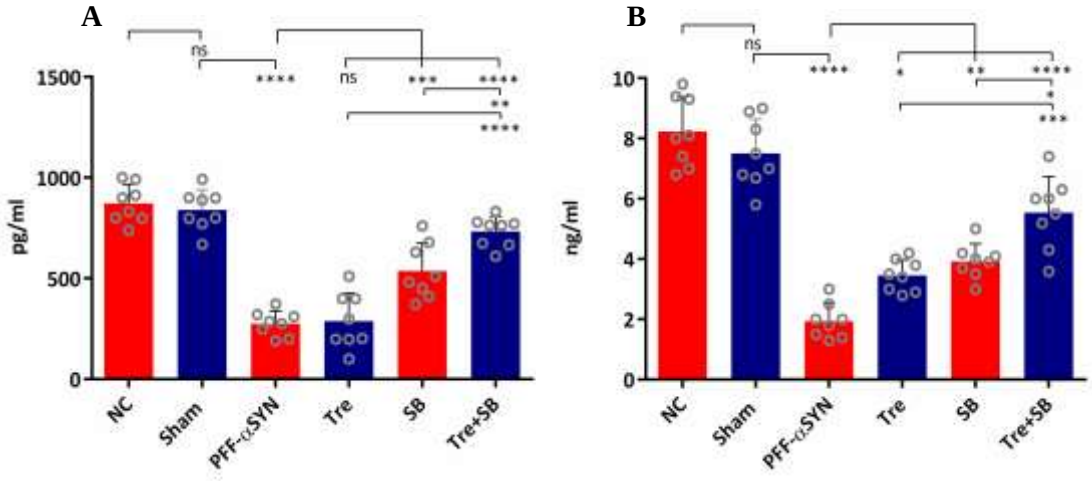

Fig. 9: (A) Effect of tre and SB on DA levels in SN: Values represents Mean ± SD, ****P≤0.0001 (Sham vs PFF α-syn); ns (PFF α-syn vs tre); ***P≤0.001 (PFF α-syn vs SB); ****P≤0.0001 (PFF α-syn vs tre+SB); ****P≤0.0001 (tre+SB vs tre); **P≤0.01 (tre+SB vs SB), F (5,42) = 51.40, P<0.0001; **(B)** Striatum DA level: ****P≤0.0001 (Sham vs PFF α-syn); *P≤0.05 (PFF α-syn vs tre); **P≤0.01 (PFF α-syn vs SB); ****P≤0.0001 (PFF α-syn vs tre+SB); ***P≤0.001 (tre+SB vs tre) *P≤0.05 (tre+SB vs SB), F (5,42) = 57.38, P<0.0001; ns: non-significant, NC: normal control.

IX. Effect of tre and SB on levels of global histone H3 acetylation

PD pathogenesis is associated with several epigenetic modifications which is also known to regulate expression of autophagy related genes. The predominant component of LBs, i.e., α-syn is known to decrease histone H3 acetylation levels in cultured cells leading to cell death[29]. Hence, we explored the global histone H3 acetylation level to assess the harmful effect of PFF α-syn and effective reversal by tre and SB. Intriguingly, we observed that reduced H3 acetylation levels was evidenced in the group of PFF α-syn when compared to the sham control group ($^{****}P\leq0.0001$), which was significantly upregulated on administration with tre, SB in alone ($^{*}P\leq0.05$ and $^{**}P\leq0.01$ respectively) and tre and SB in combination ($^{****}P\leq0.0001$). Moreover, in the combination group histone acetylation was significantly increased in comparison with tre and SB treatments in alone as $^{***}P\leq0.001$ for tre+SB vs tre and $^{**}P\leq0.01$ for tre+SB vs SB (figure 10).

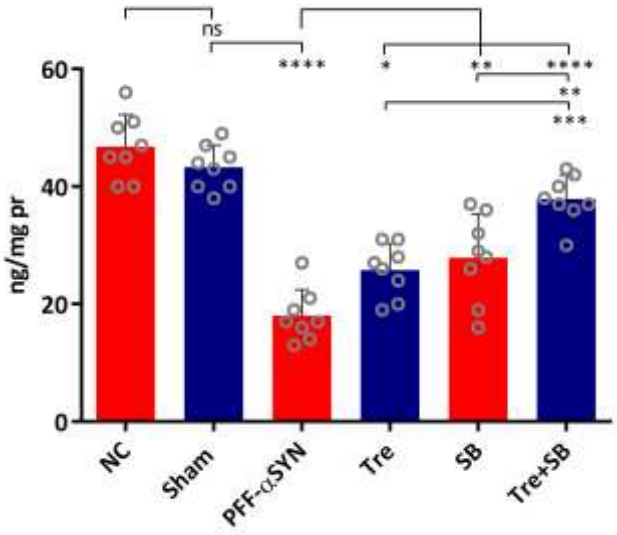

Fig. 10: Effect of tre and SB on H3 levels: Values represents Mean ± SD, $^{****}P\leq0.0001$ (Sham vs PFF α-syn); $^{*}P\leq0.05$ (PFF α-syn vs tre); $^{**}P\leq0.01$ (PFF α-syn vs SB); $^{****}P\leq0.0001$ (PFF α-syn vs tre+SB); $^{***}P\leq0.001$ (tre+SB vs tre); $^{**}P\leq0.01$ (tre+SB vs SB), F (5,42) = 38.02, P<0.0001, ns: non-significant, NC: normal control.

X. Effect of tre and SB on various mRNA expression

The initiating step in autophagosome assembly from pre-autophagic structures is orchestrated by a 60kDa protein, beclin-1. In PD, the beclin-1 level is found to reduce with increasing α-syn accumulation suggesting alterations in the process of autophagy[30]. Therefore, examining the mRNA expression of beclin-1 would provide conclusive evidence about PD progression and its effective amelioration by the respective treatments. It was observed that the PFF α-syn group had a decreased expression of beclin-1when compared with sham ($^{****}P\leq0.0001$). However, the expression level of beclin-1 was found to significantly increase with tre ($^{****}P\leq0.0001$) and SB ($^{****}P\leq0.0001$) alone and tre and SB in combination ($^{****}P\leq0.0001$) treatment when compared with disease group. Further, combination group in comparison with treatments in alone also demonstrated significant increase in the expression of beclin-1 ($^{****}P\leq0.0001$) for both tre+SB vs tre and tre+SB vs SB (figure 11a).

LC3-II is produced upon conjugation of LC3-II to phosphatidylethanolamine (PE) on the surface of nascent autophagosomes. In PD, deficiency of LC3-II to form autophagosomes might impair the overall machinery of autophagy in clearing out aggregate-prone proteins[31]. Hence, we analysed the mRNA levels of LC3-II and observed that the group with PFF α-syn had an impaired level of LC3-II when compared to sham ($^{****}P\leq0.0001$), and treatment with tre and SB alone improved the levels of LC3-II ($^{****}P\leq0.0001$). Similarly, the combined administration of tre and SB also significantly increased LC3-II expression level ($^{****}P\leq0.0001$) when compared with disease group. In addition, the combination group when compared with treatments in alone also shows a significant rise in the LC3-II expression level as $^{****}P\leq0.0001$ for both tre+SB vs tre and tre+SB vs SB (figure 11b).

Lysosomal stability and autophagy requires LAMP-2. In neurodegenerative conditions like PD, reduced levels of LAMP-2 are evidenced in LBs of the SN and also in the amygdala. Therefore, we examined the expression level of LAMP-2 to better arrive at a conclusion of the severity of PD pathogenesis and its effective reversal by the treatments. It was observed that, the PFF α-syn administration decreased the LAMP-2 expression on comparison with sham group ($^{****}P\leq0.0001$), while an improvement was observed in SB alone treated group ($^{***}P\leq0.001$). However, a marked increase in the mRNA expression level of LAMP-2 was found on administration with tre and SB in combination ($^{****}P\leq0.0001$). No significant change was observed for the group treated with tre alone. Moreover, the combination group revealed significant increase in LAMP-2 expression when compared with tre and SB in alone as $^{****}P\leq0.0001$ for both tre+SB vs tre and tre+SB vs SB (figure 11c).

TH is an enzyme mainly catalysing the rate limiting step for the synthesis of DA via formation of L-dihydroxyphenylalanine (L-DOPA). Moreover, the early depletion of TH activity and subsequent reduction in TH protein accounts for the deficiency in DA and phenotypic expression of PD[32]. However, upon analysing TH mRNA expression in the current study, a considerable decrease was observed in the PFF α-syn group when compared to the sham group ($^{****}P\leq0.0001$) followed by an enhancement in TH mRNA expression after treatment with tre (not significant) and SB ($^{****}P\leq0.0001$) in alone and with combination of tre and SB ($^{****}P\leq0.0001$). In addition, a significant increase in TH mRNA expression was found in combination group when compared to the tre and SB treatments in alone, as $^{****}P\leq0.0001$ for both tre+SB vs tre and tre+SB vs SB (figure 11d).

DAT is majorly known to regulate synaptic DA concentration in the striatum affecting locomotor activity. During PD, loss of DAT severely hampers DA clearance resulting in motor abnormalities. Upon analysing the mRNA expression levels of DAT, we observed that the PD induced group had a considerable decrease in its expression on comparison with control group ($^{****}P\leq0.0001$). However, the treatment with tre, SB in alone and their combination increased the level of DAT mRNA expression ($^{*}P\leq0.05$, $^{****}P\leq0.0001$, $^{****}P\leq0.0001$ respectively). Further, when the combination group compared with tre and SB in alone significantly elevated DAT expression as $^{****}P\leq0.0001$ for both tre+SB vs tre and tre+SB vs SB (figure 11e).

The presynaptic protein, α-syn shares a close relation with the pathogenesis of PD. From a plethora of available hypothesis linking α-syn and PD, the most common is the fact that the soluble fibrillar forms of α-syn, namely its PFF form, evokes neuronal death. Therefore, we analysed the mRNA expression level of α-syn in its native form and its effect in the PFF α-syn group and after treatment with tre and SB. The fibrillar form was found to reduce the levels of

α-syn mRNA when compared with the sham group (****P≤0.0001). Quite interestingly, we observed that α-syn expression was significantly improved after treatment with tre, SB in alone and with their combination when compared to the group administered with the toxic oligomeric form of α-syn (**P≤0.01, ****P≤0.0001, ****P≤0.0001 respectively). Moreover, when the combination group was compared with tre and SB treatments in alone revealed a significant improvement in the α-syn expression level as ****P≤0.0001 for both tre+SB vs tre and tre+SB vs SB (figure 11f).

The cytoskeletal protein MAP-2 stabilizes the microtubule assembly. The progressive loss of DA neurons is due to the formation of cytoplasmic lewy bodies (LBs) during PD. The alteration in the cellular cytoskeleton and allied aberrant neuronal transport can lead to neuronal loss. The microtubules in neuronal dendrites are stabilized with cytoskelton protein MAP-2, which is also mediates for the interaction with neighbouring neurons. Hence, we analysed the levels of MAP-2 mRNA expression in the current study and found that, there was a considerable reduction in the MAP-2 expression in the PFF α-syn group (**P≤0.01), which was efficiently reversed by the tre, SB treatment in alone and their combination (*P≤0.05, ****P≤0.0001, ****P≤0.0001 respectively). Further, the MAP-2 expression in the combination group was found significantly increased when compared with tre and SB in alone (****P≤0.0001 for both tre+SB vs tre and tre+SB vs SB) (figure 11g).

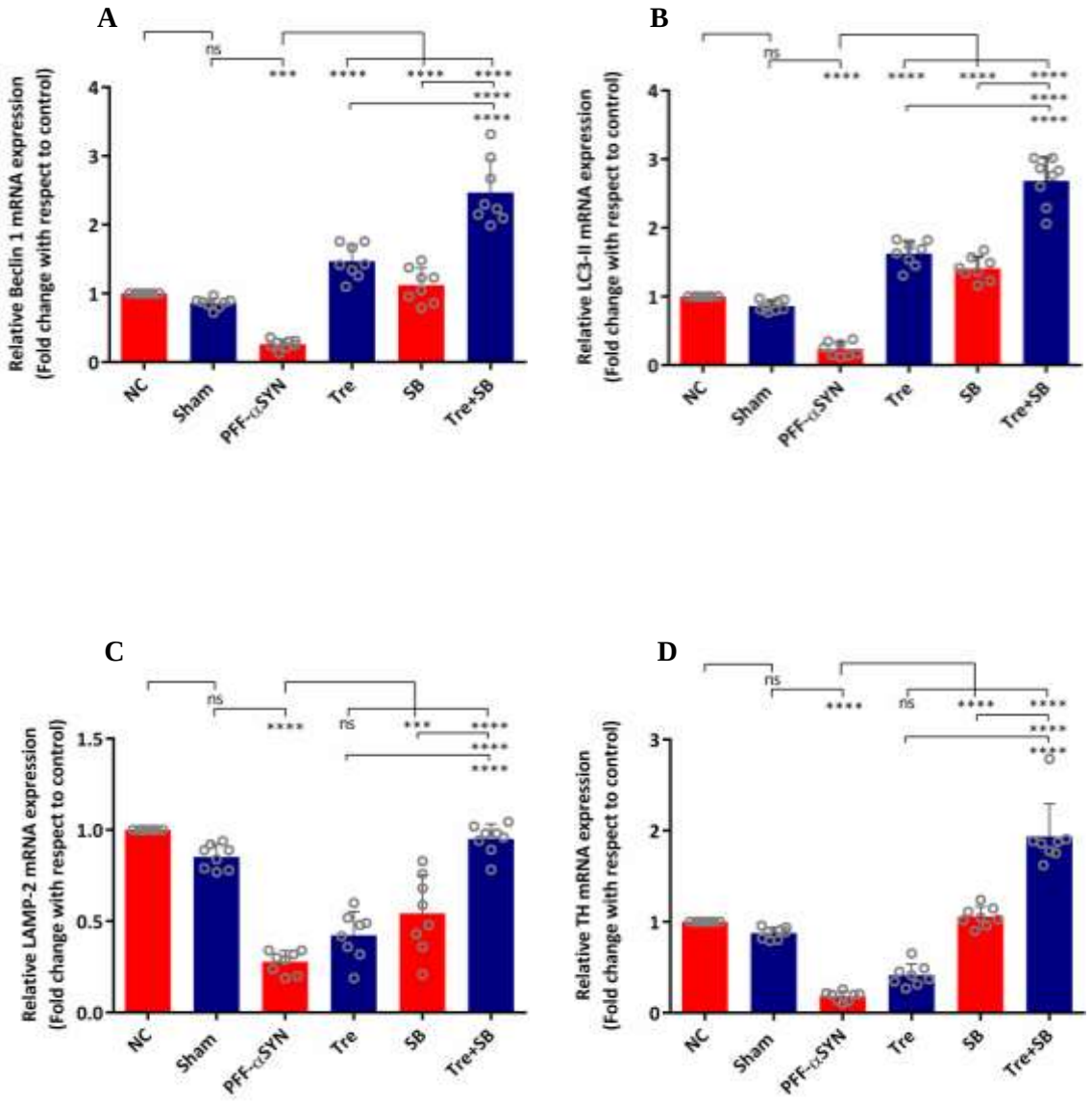

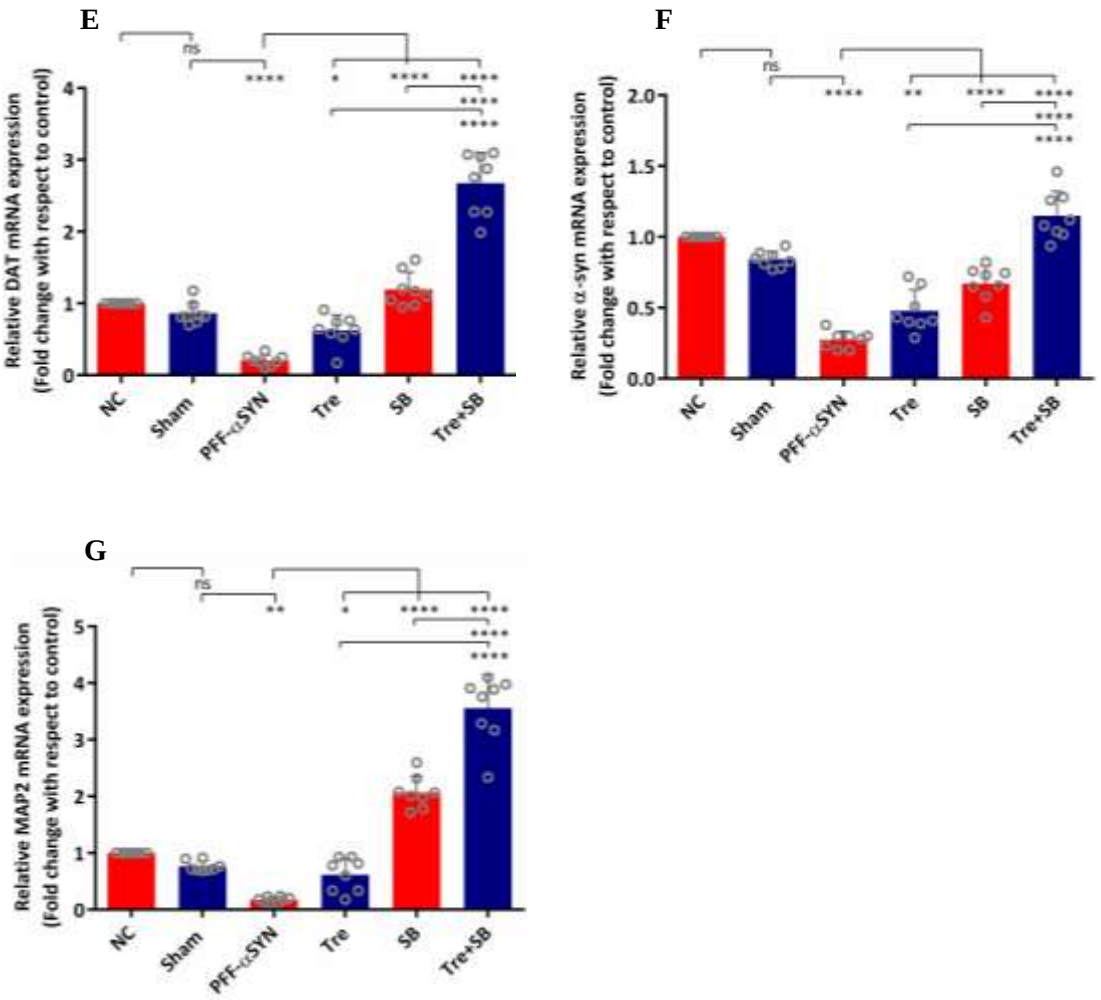

Fig. 11: (A) Effect of tre and SB on beclin-1 mRNA expression: Values represents Mean ± SD, ***P≤0.001 (Sham vs PFF α-syn); ****P≤0.0001 (PFF α-syn vs tre); ****P≤0.0001 (PFF α-syn vs SB); ****P≤0.0001 (PFF α-syn vs tre+SB); ****P≤0.0001 (tre+SB vs tre); ****P≤0.0001 (tre+SB vs SB), F (5, 42) = 73.35, P<0.0001; **(B)** LC3-II mRNA expression: Values represents Mean ± SD, ****P≤0.0001 (Sham vs. PFF α-syn); ****P≤0.0001 (PFF α-syn vs tre); ****P≤0.0001 (PFF α-syn vs SB); ****P≤0.0001 (PFF α-syn vs tre+SB); ****P≤0.0001 (tre+SB vs tre); ****P≤0.0001 (tre+SB vs SB), F (5, 42) = 165.7, P<0.0001; **(C)** LAMP-2 mRNA expression: Values represents Mean ± SD, ****P≤0.0001 (Sham vs PFF α-syn); ns (PFF α-syn vs tre), ***P≤0.001 (PFF α-syn vs SB), ****P≤0.0001 (PFF α-syn vs tre+SB); ****P≤0.0001 (tre+SB vs tre); ****P≤0.0001 (tre+SB vs SB), F (5,42) = 57.06, P<0.0001; **(D)** TH mRNA expression: Values represents Mean ± SD, ****P≤0.0001 (Sham vs PFF α-syn); ns (PFF α-syn vs tre); ****P≤0.0001 (PFF α-syn vs SB); ****P≤0.0001 (PFF α-syn vs tre+SB); ****P≤0.0001 (tre+SB vs tre); ****P≤0.0001 (tre+SB vs SB), F (5,42) = 110.6, P<0.0001; **(E)** DAT mRNA expression: Values represents Mean ± SD, ****P≤0.0001 (Sham vs PFF α-syn); *P≤0.05 (PFF α-syn vs tre); ****P≤0.0001 (PFF α-syn vs SB); ****P≤0.0001 (PFF α-syn vs tre+SB); ****P≤0.0001 (tre+SB vs tre); ****P≤0.0001 (tre+SB vs SB), F (5,42) = 106.8, P<0.0001; **(F)** α-syn mRNA expression:

Values represents Mean ± SD, ****P≤0.0001 (Sham vs PFF α-syn); **P≤0.01 (PFF α-syn vs tre); ****P≤0.0001 (PFF α-syn vs SB); ****P≤0.0001 (PFF α-syn vs tre+SB); ****P≤0.0001 (tre+SB vs tre); ****P≤0.0001 (tre+SB vs SB), F (5,42) = 70.22, P<0.0001; **(G)** Effect of tre and SB on MAP-2 mRNA expression: Values represents Mean ± SD, **P≤0.01 (Sham vs PFF α-syn); *P≤0.05 (PFF α-syn vs tre), ****P≤0.0001 (PFF α-syn vs SB); ****P≤0.0001 (PFF α-syn vs tre+SB); ****P≤0.0001 (tre+SB vs tre); ****P≤0.0001 (tre+SB vs SB), F (5,42) = 141.1, P<0.0001, ns: non-significant, NC: normal control.

XI. Western blot analysis

SQSTM1 is a cytoplasmic protein detectable in inclusion bodies of protein aggregates, responsible for degradation of ubiquitinated substrates. Here, we examined SQSTM1 levels in the SN region of the brain and observed faint bands in the PFF α-syn group which was reversed after tre and SB treatment where the single treatment of the drugs increased SQSTM1 protein levels and the combination treatment significantly up regulated the SQSTM1 protein level when compared to the PFF α-syn group which might be attributable to the capacity of tre to increase SQSTM1 levels[33]. Moreover, when the combination group was compared with treatments in alone, the SQSTM1 protein level was significantly increased as *P≤0.05, for tre+SB vs tre and *P≤0.05, for tre+SB vs SB (fig 12A and 12B). The expression level of SQSTM1 correlated with other autophagic flux markers, which limits assessment of SQSTM1 level in understanding autophagy mechanism. Moreover, SQSTM1 is degraded by autophagy as well as proteasome system and this proteasome inhibition can increase the SQSTM1 level although proteasome inhibition can increase autophagosome[34,35]. The SQSTM1 contains domain which can interact with many signalling moieties which points out its other function. The studies conducted by Abokyi S demonstrated that tre treatment in human retinal pigment epithelial cells was found to increase SQSTM1 level; however the expression level was much higher when co-incubated with chloroquine indicating the increased synthesis of SQSTM1 by tre[36]. Considering the level of SQSTM1 is not sufficient to assess autophagy hence in parallel to this, the expression of LC3-II was also checked. Cytosolic LC3-I undergoes post-translational modification from endogenous LC3 which is then converted to LC3-II that is attached to autophagosome membranes[37]. LC3-II (PE-conjugated) has a larger molecular weight than that of LC3-I (16 kDa) which is why on SDS-PAGE due to its extreme hydrophobicity, LC3-II migrates faster than LC3-I reaching approximately 15kDa as seen in the image. Tre and SB is known to upregulate the protein levels of LC3-II[38,39] which was consistent with our findings where we observed a significant up-regulation in the tre and SB treatment in alone as well as in the combination group in contrast to that of the disease group (**P≤0.01, *P≤0.05, **P≤0.01 respectively). The increase in the LC3-II protein levels were observed to be statistically similar for the drugs treated alone and in combination (fig 12A and 12C).

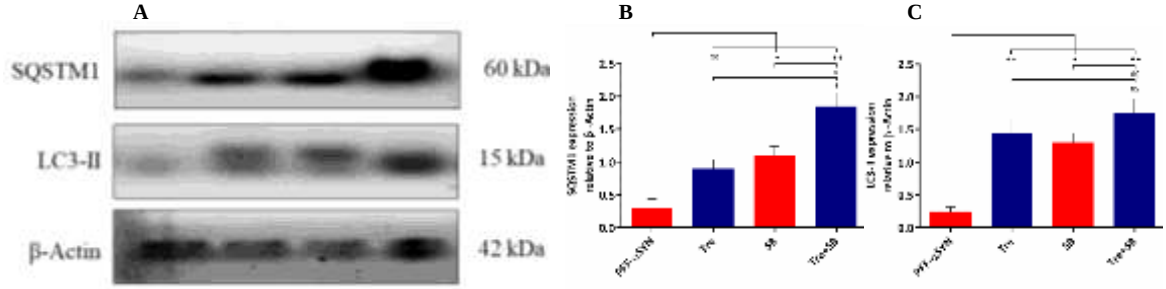

Fig. 12: (A) Western blot for SQSTM1, LC3-II on treatment with tre and SB, (lane 1: PFF α-syn, lane 2: tre, lane 3: SB, lane 4: tre+SB); **(B)** Quantified data for SQSTM1 expression: values represents Mean ± SD, ns (PFF α-syn vs Tre); $^{*}P \leq 0.05$ (PFF α-syn vs SB); $^{**}P \leq 0.01$ (PFF α-syn vs Tre+SB); $^{*}P \leq 0.05$ (tre+SB vs tre); $^{*}P \leq 0.05$ (tre+SB vs SB), $F = 31.16$, $P \leq 0.0031$, **(C)** Quantified data for LC3-II expression: $^{**}P \leq 0.01$ (PFF α-syn vs Tre); $^{*}P \leq 0.05$ (PFF α-syn vs SB); $^{**}P \leq 0.01$ (PFF α-syn vs Tre+SB); ns (tre+SB vs tre); ns (tre+SB vs SB), $F = 29.61$, $P \leq 0.0034$.

XII. Histopathological analysis

Along with motor abnormalities observed during the assessment of the behavioural parameters, the PFF α-syn group presented with morphological alterations, particularly in the SN region of the brain. The brain sections stained with H&E revealed the presence of healthy/ normal neurons in SN region in the sham and the normal control group. The ratio of healthy neurons was found to be approximately equivalent for both normal and sham control group. The normal neurons were observed as spherical with slight oval shaped nucleus, a nucleolus, and a clear cytoplasm (represented with yellow arrows). On the other hand, the PFF α-syn group had decreased neuronal density, increased pyknotic and darkly stained neurons, shrunken neurons and slight vacuolization in the SN region (represented with red arrows). The treatment with tre and SB alone could faintly ameliorate the PFF α-syn induced neuronal pyknosis and loss of neuronal density ($^{*}P \leq 0.05$ for SB; Supplementary figure 4). However, a significant reduction in the pyknotic neurons and improved neuronal distribution were observed in combination treatment with tre and SB ($^{**}P \leq 0.01$). Further, when the combination group was compared with treatments in alone, the percentage neurodegenerative area was tend to decrease significantly with tre ($^{*}P \leq 0.05$, tre+SB vs tre) but not with SB (figure 13A and B).

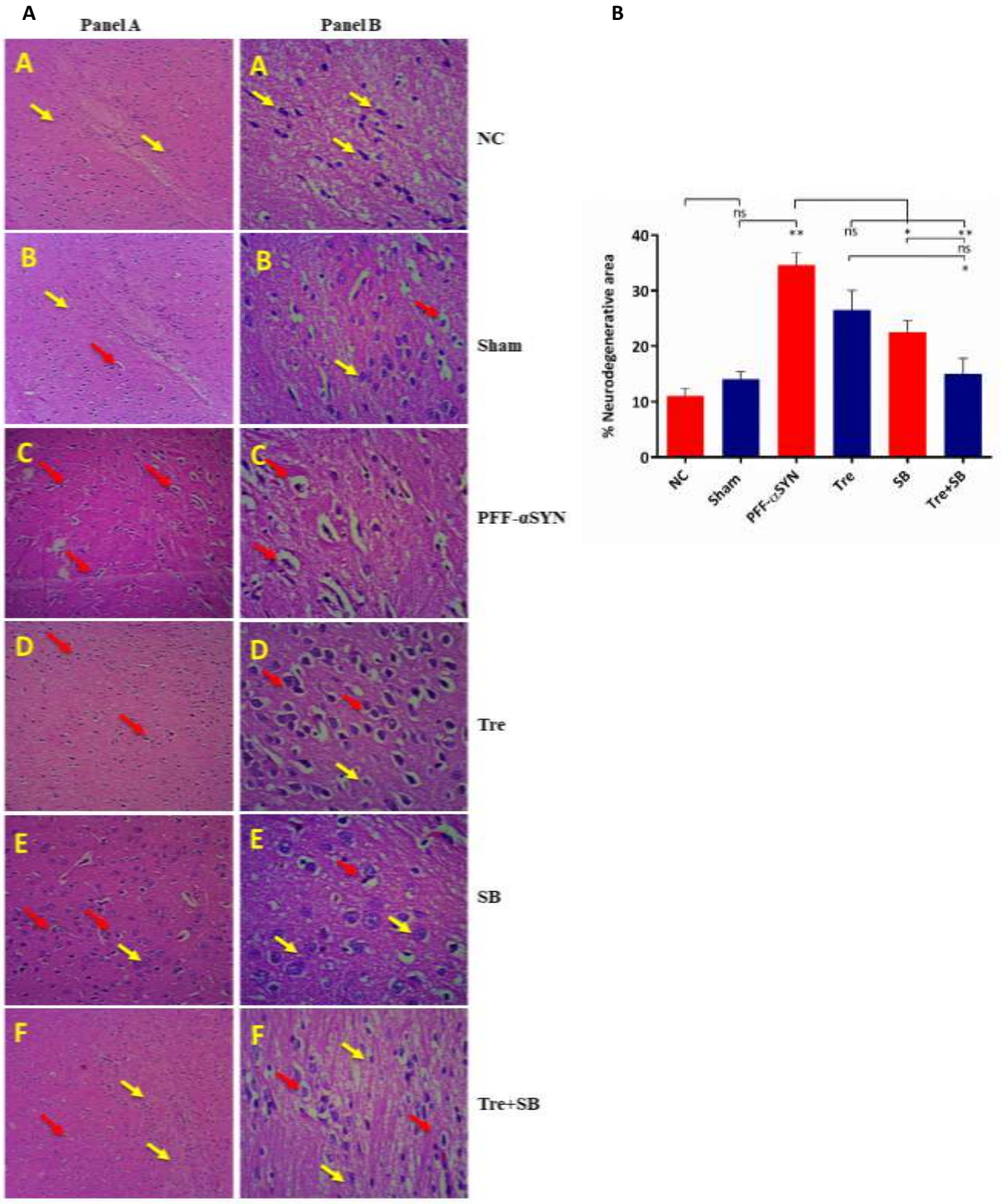

Fig. 13 (A): H & E analysis of the SN region of the brain at 10X (Panel A) and 40X magnification (Panel B). As observed in 40X magnification, the figure A and B displays the presence of spherical neuronal bodies with a greater density indicated by yellow arrows, C represents darkly stained and shrunken neurones with slight vacuolization, D and E seems to revive the loss of neurones with less darkly stained and shrunken neurones as indicated by yellow arrows and F represents a dense population of neurones with spherical/oval shaped

nucleus indicating the presence of healthy neurones. (A: NC; B: Sham; C: PFF-Asyn; D: tre; E: SB; F: tre+SB). **(B)** Quantified data for H & E analysis of the SN region of the brain: Analysis of the degenerative area using image J software revealed $^{**}P \leq 0.01$ (Sham vs PFF α-syn); ns (PFF α-syn vs Tre); $^{*}P \leq 0.05$ (PFF α-syn vs SB); $^{**}P \leq 0.01$ (PFF α-syn vs Tre+SB); $^{*}P \leq 0.05$ (tre+SB vs tre); ns (tre+SB vs SB), $F(5,6) = 28.28$, $P = 0.0004$, Values represented as Mean ± SD, ns: non-significant, NC: normal control.

XIII. Immunofluorescence analysis

a. Estimation of astrogliosis and microgliosis: No significant differences were observed in terms of immunoreactivity for the normal and sham control group. Thus, only the sham group was kept as control group. Moreover, from the behavioural, mRNA expression level and histochemical analysis we found that the animals treated with combination of tre and SB significantly improved the PD condition. Hence, we have chosen the combination group for immunolabelling to further confirm its efficacy in ameliorating PD pathology.

Post-mortem analysis has revealed the importance of microgliosis and astrogliosis in PD. Examining the extent of inflammation in the microglia and astrocytes could provide a better explanation on the severity of PD pathology. Autophagy stimulation and suppression of hepatic inflammatory chain by tre have attracted the attention of researchers[40–42]. Additionally, the antioxidant and lipid peroxidation activity in tre supplemented diet of cow milk were improved[43,44]. Moreover, a study conducted by chen et al., on mice model of inflammatory bowel disease induced by TNBS, the SB treatment prevented inflammation and maintained epithelial barrier integrity[45].

GFAP, a protein mainly known to regulate astrocyte function and morphology was used as an effective astrogliosis marker and IBA-1, a microglia specific calcium-binding protein involved in phagocytosis in activated microglia was used to measure the extent of microgliosis in the PD brain. Quite interestingly, we observed that there was an increase in the number of GFAP cells (green) ($^{**}P \leq 0.01$) and IBA-1 (red) in the PFF α-syn group ($^{*}P \leq 0.05$) and a gradual decrease in the total number of GFAP cells in the treated group with combination of tre and SB ($^{**}P \leq 0.01$) (figure 14) and also IBA-1 cells ($^{*}P \leq 0.05$).

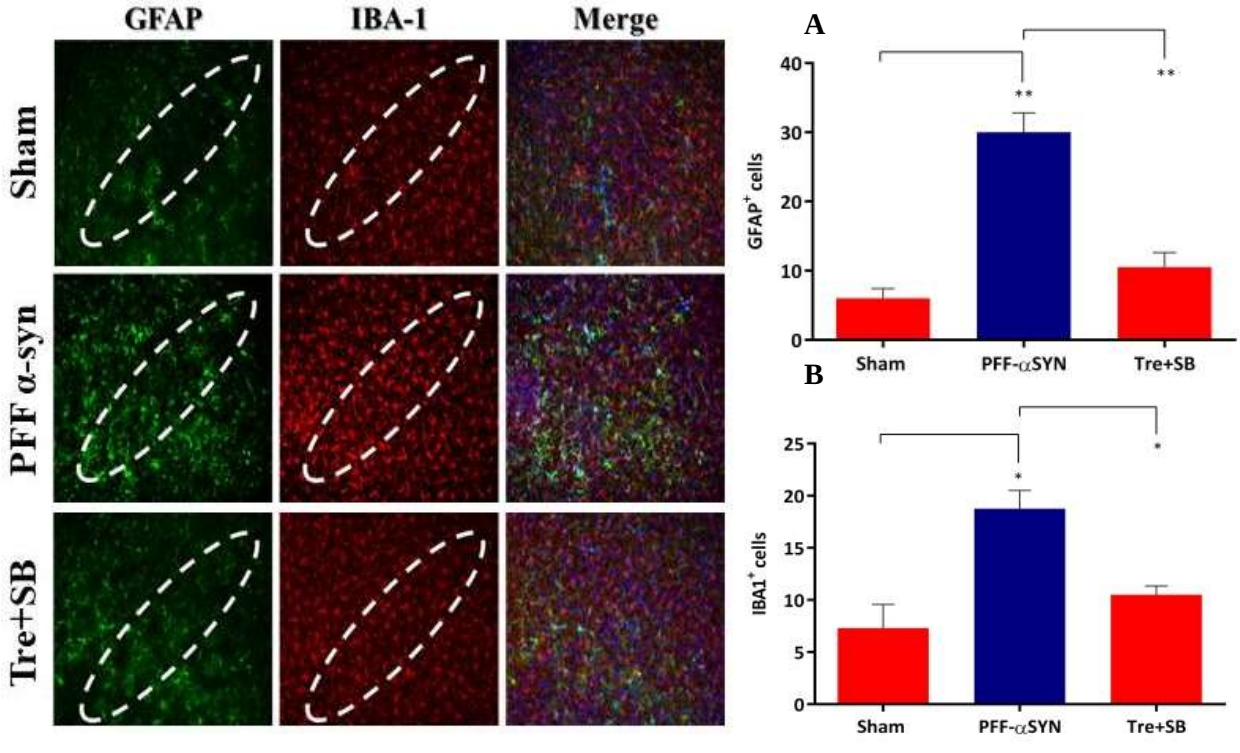

Fig. 14: Increased astrogliosis (GFAP, green) and microgliosis (IBA-1, red) in the SN after striatal seeding of PFF α-syn and effective reversal after treatment with tre and SB. Bar graph represents Mean ± SD. **(A)** $GFAP^+$ cells: $^{**}P \leq 0.01$ (NC vs PFF α-syn); $^{**}P \leq 0.01$ (PFF α-syn vs tre+SB), F (2, 3) = 67.34, P = 0.0032, **(B)** $IBA1^+$ cells: $^{*}P \leq 0.05$ (NC vs PFF α-syn); $^{*}P \leq 0.05$ (PFF α-syn vs tre+SB), F (2,3) = 23.36, P = 0.0148, ns: non-significant, NC: normal control.

b. **Estimation of DA neuronal loss:** During PD, there is a substantial loss particularly in the TH, the rate limiting enzyme in DA synthesis along with the loss of NeuN. In PD, NeuN is used to estimate the exact loss of nigral DA neurones that can be effectively differentiated from TH loss alone. After performing IFC for the SN region to detect TH and NeuN positive cells, it was observed that the percentage (%) positive cells for TH and NeuN was quite low in the PFF α syn group which was restored after treatment with the combination of tre and SB ($^{*}P \leq 0.05$) (figure 15).

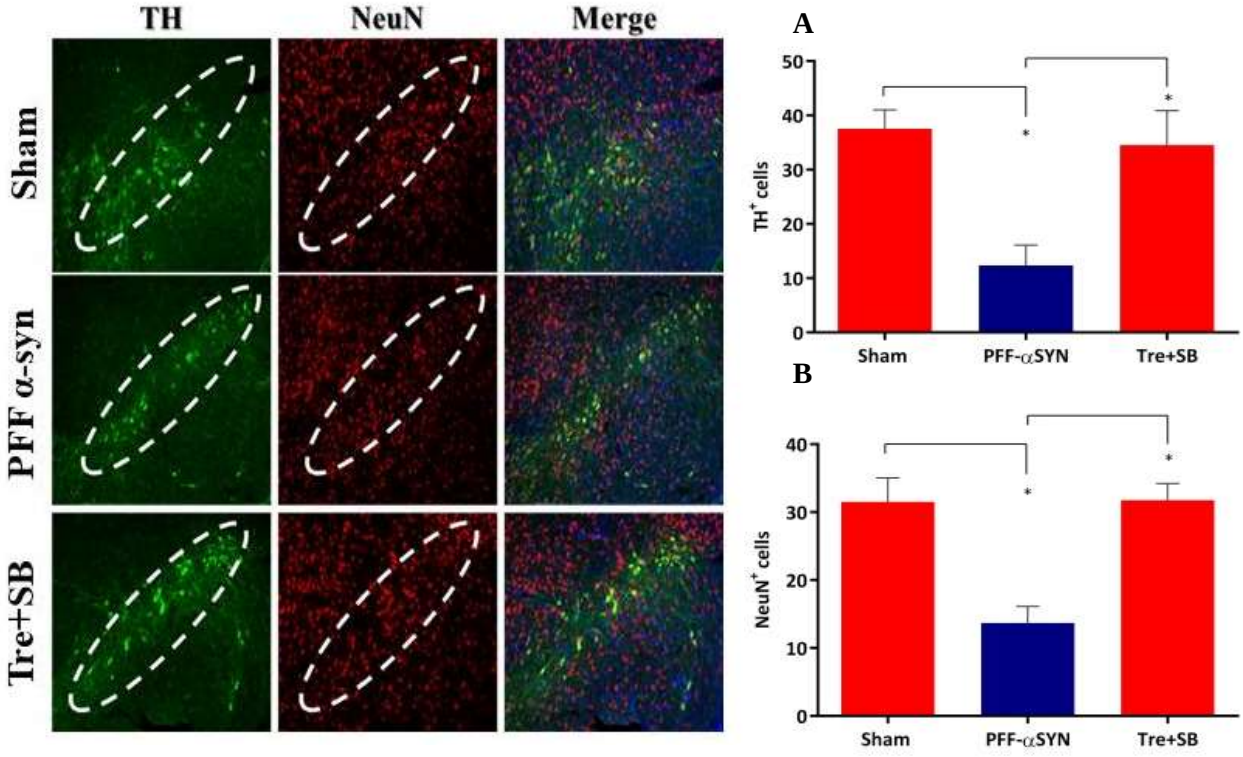

Fig. 15: Increased DA neurodegeneration as evidenced after staining with TH (green) and NeuN (Red) in the SN after striatal seeding of PFF α-syn and effective reversal after treatment with tre and SB. Bar graph represents Mean ± SD. **(A)** TH^+ cells: $^{*}P \leq 0.05$ (NC vs PFF α-syn); $^{*}P \leq 0.05$ (PFF α-syn vs tre+SB), F (2,3)=16.89, P=0.0233, **(B)** $NeuN^+$ cells: $^{*}P \leq 0.05$ (NC vs PFF α-syn); $^{*}P \leq 0.05$ (PFF α-syn vs tre+SB), F (2,3) = 26.33, P = 0.0125, ns: non-significant, NC: normal control.

c. **Estimation of phosphorylated α-syn (Serine 129):** PD pathogenesis undergo various post-translational modifications to α-syn, one among them is the phosphorylated α-syn (p α-syn) which is known to enhance α-syn toxicity both *in-vitro* and *in-vivo*. Therefore, we wanted to see whether there is any change in p α-syn levels counterstained with TH before and after treatment. The PFF α-syn group had a high intensity of p α-syn (red) on comparison with the

sham group (*P≤0.05). Conversely, almost no p α-syn signal was detected in the group administered with both tre and SB (*P≤0.05) with an increased count of positive cells for TH (figure 16).

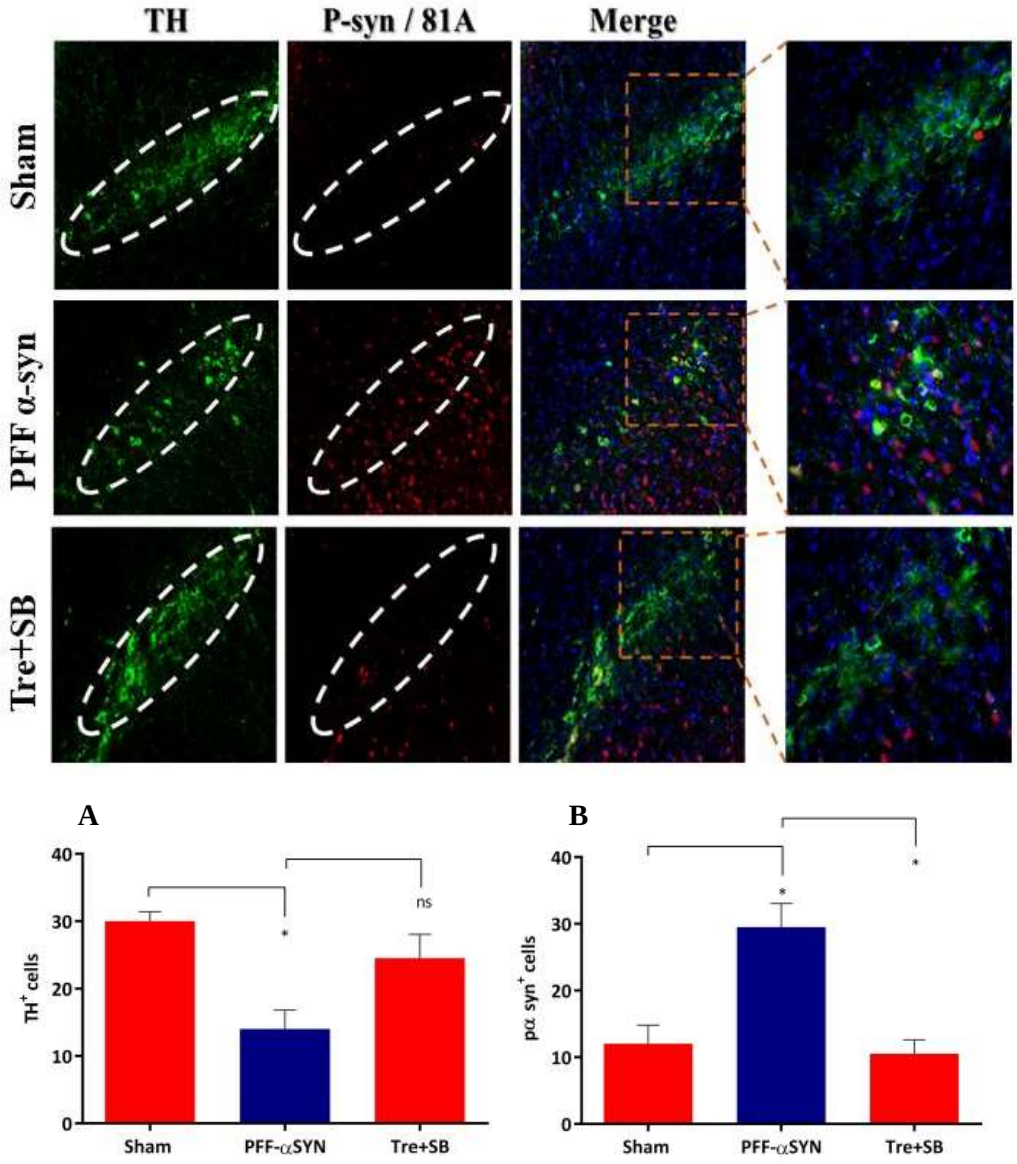

Fig. 16: Increased levels of phosphorylated α-syn (S129) (red) and decreased levels of TH (green) in the SN after striatal seeding of PFF α-syn and effective reversal after treatment with tre and SB. Bar graph represents Mean ± SD. (A) TH^+ cells: *P≤0.05 (sham vs PFF α-syn); ns (PFF α-syn vs tre+SB), F (2, 3) = 17.62, P = 0.0220, (B) $P\text{-}syn^+$ cells: *P≤0.05 (NC vs PFF α-syn); *P≤0.05 (PFF α-syn vs tre+SB), F (2, 3) = 26.78, P = 0.0122, ns: non-significant, NC: normal control.

Discussion

Complete therapeutic cure to halt the pathological progression of PD has time and again failed to reach the market and continues to emerge as a global threat. Symptomatic management with

a combination of levodopa and carbidopa are the only successful hope by far. Traditionally, PD was believed to affect motor functions of an individual due to DA neuronal loss particularly in the SN region of the brain. However, insights into recent research has brought into limelight certain non-motor symptoms, mainly cognitive disturbances that might also precede the occurrence of PD. DA neuron loss is likely to occur due to an abnormal misfolding of the oligomeric form of α syn, notably the PFF form.

The actual causal factor for this misfolding remains largely unknown, but in order to maintain a healthy neuronal environment removing these misfolded proteins with time is crucial, which throws light on autophagy, a self-conserved mechanism that can eliminate damaged and misfolded proteins governing homoeostasis in the body. But as neurodegeneration progresses, autophagy becomes dysfunctional and unable to clear out misfolded proteins, hence, autophagy activation has yielded promising results in several pre-clinical models of neurodegeneration. During PD, administration of tre to rats has resulted in successful neuroprotection, although the mechanism behind this neuroprotection is till surrounded by a lot of controversies. Nevertheless, continuous research has shed some light on the mechanism unravelling a novel direction to neuroprotection elicited by tre. Epigenetic modifications resulting during the pathological progression of PD, notably post translational histone modifications has the potential to regulate the expression of autophagy related genes. This theory in itself motivated our current study where we investigated the neuroprotective efficacy of a combination of tre and SB to ameliorate PD pathology in a PFF α syn model in rats. Tre and SB have been known as a kind of short chain fatty acid (SCFA), which is a by-product of microbial fermentation. Several previous studies described that treatment of SCFA, e.g., SB, or a mixture of SCFA aggravates neuroinflammation and motor deficits in MPTP mice model and α-syn overexpressing mice model[46,47]. Works by others have suggested the opposite, which revealed that the treatment of tre ameliorated the pathology in ALS/ Huntington mice model[48,49]. However, in the current work we observed that as compared to the combination treatment, treatment with tre alone could not ameliorate PD pathology upto a statistically significant level hinting towards the possibility that its protective effects are not only mediated via SCFA. Tre majorly functions as a protein stabiliser with autophagy activation as its secondary pharmacological function. In a transgenic (tg) mouse model of Huntington disease (HD), the tre administered orally enhanced motor dysfunction and improved lifespan. With tre administration, superoxide dismutase 1 (SOD1) mutant tg mice had a slightly longer lifetime and improved neuronal survival. In the brains of Parkin-/-/TauVLW mice, phosphorylated taupositive neuritic plaques and astrogliosis were significantly reduced. Tre inhibited the reduction of striatal DA levels and prevented gliosis in the MPTP mouse model of PD[50]. However, the neuroprotective efficacy of tre to ameliorate PFF α-syn induced PD have not yet been explored and the results of the present work clearly stated that as compared to tre alone, its combination with SB elicits much pronounced neuroprotective efficacy in PFF α-syn induced rat model of PD.

First, we started by examining a battery of behavioural abnormalities, in the PFF α syn rats and after each of the respective treatments. Based on the results obtained, it was fairly visible that

the animals induced with PFF α syn had significant motor abnormalities both in the rotarod test and NBW test when compared to the control groups. These abnormalities were reversed after treatment with a combination of tre and SB. Open field test was used to rule out any locomotor abnormality the animal might be suffering due to induction of the disease and its response after providing the respective treatment. Here, we observed that the disease group had a lower latency of distance travelled as compared to the group treated with the combination of tre and SB. Lastly, we went for determining any cognitive disturbance which might occur during PD and for that we tested the animals using NOR and NOL test. All the animals injected with PFF α syn alone were found to have cognitive discrepancy as compared to the control groups whereas the treated group both with tre and SB revealed considerable improvement. For all the tested behavioural parameters, the combination group receiving treatment with both tre and SB had a statistically significant improvement on the behavioural outcome of all the PD induced rats.

Secondly, we investigated the levels of relevant biochemical markers namely, IL-1, IL-6, TNF-α, CRP, DA, BDNF and global histone H3 acetylation with available ELISA kits. It was observed that levels of IL-1, IL-6, TNF- α and CRP considerably upregulated in the PFF α syn group and significantly improved after treatment with the combination of tre and SB. Likewise, the expression of BDNF, DA and H3 acetylation downregulated in the PFF α syn group which significantly upregulated on treatment with the combination of tre and SB.

The analysis of gene expression level of certain genes also revealed similar results whereby we found that the mRNA expression of genes like beclin-1, LC3-II, LAMP-2, the three most important determinants for the process of autophagy or autophagy induction considerably downregulated in the PFF α syn group alone, however, interestingly the expression level of these genes improved after administration of the combination of tre and SB. Moreover, after the analysis of α syn, DAT, TH and MAP-2 we could conclusively state that the treatment group with both tre and SB had a fairly potent effect even on the expression level of proteins affected most during PD pathology.

Additionally, histopathological analysis of the majorly affected area of the brain during PD, SN revealed heavily degenerated and pyknotic neurones in the group with PFF α syn alone which could be reversed after administration of a combination of tre and SB where it was observed that there was less pyknotic neuronal count with less amount of darkly stained neurons.

Lastly, IFC staining for the SN region of the brain exposed improved results with the combination group, for instance, co-staining of TH with NeuN showed that the group with PFF α syn had a lower positive cell count for TH staining (green) as well as for the NeuN staining (red) on comparison with the sham control group which was reversed on administration with both tre and SB. Similarly, upon counter staining of GFAP (green) with IBA1 (red), we observed that inflammation in the microglia and astrocytes were quite high for the PFF α syn group and low for the group receiving treatment with both tre and SB. Lastly, we wanted to see if PFF α syn induction could affect phosphorylated α syn (p α syn) level and it was seen that

there was a considerable up-regulation of p α syn in the PFF α syn group. However, a significant downregulation of p α syn was seen in the groups treated with both tre and SB.

Impact of the research in the advancement of knowledge

PD is increasingly becoming a globally dominated neurological disorder with an urgent need for newer therapeutic targets for complete therapeutic cure. Tre and SB are considerably safer drugs for oral administration with limited side effects which can also be available in several dietary regimen of our day to day life. Preclinical findings from the current study inflict a positive result for mitigation of PD pathology caused by the most toxic form of α-syn. Hence, with greater amount of studies in the future, the combination of both these drugs can emerge as successful therapeutic candidates for PD.

Conclusion

Neurodegenerative disorders like PD have cost an enormous burden to the society as the exact pathogenesis remains elusive. In the current study, we investigated the potency of tre, an autophagy inducer and SB, a pan HDAC inhibitor in ameliorating PD pathology exacerbated by PFF α-syn. Although extensive studies are still mandatory to clearly substantiate these findings, but preclinical findings in the present study have effectively concluded that tre and SB may prove to be a very powerful combination and can be considered as effective therapeutic candidates for future clinical trials in PD.

References

(1) Pringsheim, T.; Jette, N.; Frolkis, A.; Steeves, T. D. L. The Prevalence of Parkinson's Disease: A Systematic Review and Meta-Analysis. *Mov. Disord.* **2014**, *29* (13), 1583–1590.

(2) Parkinson, J. An Essay on the Shaking Palsy. *J. Neuropsychiatry Clin. Neurosci.* **2002**, *14* (2), 223–236.

(3) El-Agnaf, O. M. A.; Salem, S. A.; Paleologou, K. E.; Cooper, L. J.; Fullwood, N. J.; Gibson, M. J.; Curran, M. D.; COURT, J. A.; MANN, D. M. A.; IKEDA, S.-I.; others. α-Synuclein Implicated in Parkinson's Disease Is Present in Extracellular Biological Fluids, Including Human Plasma. *FASEB J.* **2003**, *17* (13), 1945–1947.

(4) Irwin, D. J.; Lee, V. M.-Y.; Trojanowski, J. Q. Parkinson's Disease Dementia: Convergence of α-Synuclein, Tau and Amyloid-β Pathologies. *Nat. Rev. Neurosci.* **2013**, *14* (9), 626.

(5) Poewe, W.; Seppi, K.; Tanner, C. M.; Halliday, G. M.; Brundin, P.; Volkmann, J.; Schrag, A.-E.; Lang, A. E. Parkinson Disease. *Nat. Rev. Dis. Prim.* **2017**, *3*, 17013.

(6) e Silva, A. M.; Geldsetzer, F.; Holdorff, B.; Kielhorn, F. W.; Balzer-Geldsetzer, M.; Oertel, W. H.; Hurtig, H.; Dodel, R. Who Was the Man Who Discovered the "Lewy Bodies"? *Mov. Disord.* **2010**, *25* (12), 1765–1773.

(7) Spillantini, M. G.; Schmidt, M. L.; Lee, V. M.-Y.; Trojanowski, J. Q.; Jakes, R.; Goedert, M. α-Synuclein in Lewy Bodies. *Nature* **1997**, *388* (6645), 839–840.

(8) Maroteaux, L.; Campanelli, J. T.; Scheller, R. H. Synuclein: A Neuron-Specific Protein Localized to the Nucleus and Presynaptic Nerve Terminal. *J. Neurosci.* **1988**, *8* (8), 2804–2815.

(9) Dauer, W.; Przedborski, S. Parkinson's Disease: Mechanisms and Models. *Neuron* **2003**, *39* (6), 889–909.

(10) Beach, T. G.; Adler, C. H.; Lue, L.; Sue, L. I.; Bachalakuri, J.; Henry-Watson, J.; Sasse, J.; Boyer, S.; Shirohi, S.; Brooks, R.; others. Unified Staging System for Lewy Body Disorders: Correlation with Nigrostriatal Degeneration, Cognitive Impairment and Motor Dysfunction. *Acta Neuropathol.* **2009**, *117* (6), 613–634.

(11) Luk, K. C.; Kehm, V. M.; Zhang, B.; O'Brien, P.; Trojanowski, J. Q.; Lee, V. M. Y. Intracerebral Inoculation of Pathological α-Synuclein Initiates a Rapidly Progressive Neurodegenerative α-Synucleinopathy in Mice. *J. Exp. Med.* **2012**, *209* (5), 975–986.

(12) Cuervo, A. M.; Stefanis, L.; Fredenburg, R.; Lansbury, P. T.; Sulzer, D. Impaired Degradation of Mutant α-Synuclein by Chaperone-Mediated Autophagy. *Science (80-.).* **2004**, *305* (5688), 1292–1295.

(13) Spencer, B.; Potkar, R.; Trejo, M.; Rockenstein, E.; Patrick, C.; Gindi, R.; Adame, A.; Wyss-Coray, T.; Masliah, E. Beclin 1 Gene Transfer Activates Autophagy and Ameliorates the Neurodegenerative Pathology in α-Synuclein Models of Parkinson's and Lewy Body Diseases. *J. Neurosci.* **2009**, *29* (43), 13578–13588.

(14) Felice, V. D.; Quigley, E. M.; Sullivan, A. M.; O'Keeffe, G. W.; O'Mahony, S. M. Microbiota-Gut-Brain Signalling in Parkinson's Disease: Implications for Non-Motor Symptoms. *Parkinsonism Relat. Disord.* **2016**, *27*, 1–8.

(15) Tanji, K.; Miki, Y.; Maruyama, A.; Mimura, J.; Matsumiya, T.; Mori, F.; Imaizumi, T.; Itoh, K.; Wakabayashi, K. Trehalose Intake Induces Chaperone Molecules along with Autophagy in a Mouse Model of Lewy Body Disease. *Biochem. Biophys. Res. Commun.* **2015**, *465* (4), 746–752.

(16) Martano, G.; Gerosa, L.; Prada, I.; Garrone, G.; Krogh, V.; Verderio, C.; Passafaro, M. Biosynthesis of Astrocytic Trehalose Regulates Neuronal Arborization in Hippocampal Neurons. *ACS Chem. Neurosci.* **2017**, *8* (9), 1865–1872.

(17) Béranger, F.; Crozet, C.; Goldsborough, A.; Lehmann, S. Trehalose Impairs Aggregation of PrPSc Molecules and Protects Prion-Infected Cells against Oxidative Damage. *Biochem. Biophys. Res. Commun.* **2008**, *374* (1), 44–48.

(18) Casarejos, M. J.; Solano, R. M.; Gomez, A.; Perucho, J.; De Yébenes, J. G.; Mena, M. A. The Accumulation of Neurotoxic Proteins, Induced by Proteasome Inhibition, Is Reverted by Trehalose, an Enhancer of Autophagy, in Human Neuroblastoma Cells. *Neurochem. Int.* **2011**, *58* (4), 512–520.

(19) Ferguson, S. A.; Law, C. D.; Sarkar, S. Chronic MPTP Treatment Produces Hyperactivity in Male Mice Which Is Not Alleviated by Concurrent Trehalose Treatment. *Behav. Brain Res.* **2015**, *292*, 68–78.

(20) Sarkar, S.; Chigurupati, S.; Raymick, J.; Mann, D.; Bowyer, J. F.; Schmitt, T.; Beger, R. D.; Hanig, J. P.; Schmued, L. C.; Paule, M. G. Neuroprotective Effect of the Chemical Chaperone, Trehalose in a Chronic MPTP-Induced Parkinson's Disease Mouse Model. *Neurotoxicology* **2014**, *44*, 250–262. https://doi.org/10.1016/j.neuro.2014.07.006.

(21) He, Q.; Koprich, J. B.; Wang, Y.; Yu, W.; Xiao, B.; Brotchie, J. M.; Wang, J. Treatment with Trehalose Prevents Behavioral and Neurochemical Deficits Produced in an AAV α-Synuclein Rat Model of Parkinson's Disease. *Mol. Neurobiol.* **2016**, *53* (4), 2258–2268.

(22) Füllgrabe, J.; Lynch-Day, M. A.; Heldring, N.; Li, W.; Struijk, R. B.; Ma, Q.; Hermanson, O.; Rosenfeld, M. G.; Klionsky, D. J.; Joseph, B. The Histone H4 Lysine 16 Acetyltransferase HMOF Regulates the Outcome of Autophagy. *Nature* **2013**, *500* (7463), 468–471.

(23) Wend, P.; Fang, L.; Zhu, Q.; Schipper, J. H.; Loddenkemper, C.; Kosel, F.; Brinkmann, V.; Eckert, K.; Hindersin, S.; Holland, J. D.; others. Wnt/β-Catenin Signalling Induces MLL to Create Epigenetic Changes in Salivary Gland Tumours. *EMBO J.* **2013**, *32* (14), 1977–1989.

(24) Schotta, G.; Lachner, M.; Sarma, K.; Ebert, A.; Sengupta, R.; Reuter, G.; Reinberg, D.; Jenuwein, T. A Silencing Pathway to Induce H3-K9 and H4-K20 Trimethylation at Constitutive Heterochromatin. *Genes Dev.* **2004**, *18* (11), 1251–1262.
(25) Marques, S.; Outeiro, T. F. Epigenetics in Parkinson's and Alzheimer's Diseases. In *Epigenetics: Development and Disease*; Springer, 2013; pp 507–525.
(26) Monti, B.; Gatta, V.; Piretti, F.; Raffaelli, S. S.; Virgili, M.; Contestabile, A. Valproic Acid Is Neuroprotective in the Rotenone Rat Model of Parkinson's Disease: Involvement of α-Synuclein. *Neurotox. Res.* **2010**, *17* (2), 130–141.
(27) Sharma, S.; Taliyan, R.; Singh, S. Beneficial Effects of Sodium Butyrate in 6-OHDA Induced Neurotoxicity and Behavioral Abnormalities: Modulation of Histone Deacetylase Activity. *Behav. Brain Res.* **2015**, *291*, 306–314.
(28) Siuda, J.; Patalong-Ogiewa, M.; Żmuda, W.; Targosz-Gajniak, M.; Niewiadomska, E.; Matuszek, I.; J\kedrzejowska-Szypułka, H.; Rudzińska-Bar, M. Cognitive Impairment and BDNF Serum Levels. *Neurol. Neurochir. Pol.* **2017**, *51* (1), 24–32.
(29) Kontopoulos, E.; Parvin, J. D.; Feany, M. B. α-Synuclein Acts in the Nucleus to Inhibit Histone Acetylation and Promote Neurotoxicity. *Hum. Mol. Genet.* **2006**, *15* (20), 3012–3023.
(30) Xilouri, M.; Vogiatzi, T.; Vekrellis, K.; Park, D.; Stefanis, L. Abberant α-Synuclein Confers Toxicity to Neurons in Part through Inhibition of Chaperone-Mediated Autophagy. *PLoS One* **2009**, *4* (5), e5515.
(31) Higashi, S.; Moore, D. J.; Minegishi, M.; Kasanuki, K.; Fujishiro, H.; Kabuta, T.; Togo, T.; Katsuse, O.; Uchikado, H.; Furukawa, Y.; others. Localization of MAP1-LC3 in Vulnerable Neurons and Lewy Bodies in Brains of Patients with Dementia with Lewy Bodies. *J. Neuropathol. Exp. Neurol.* **2011**, *70* (4), 264–280.
(32) Blanchard-Fillion, B.; Souza, J. M.; Friel, T.; Jiang, G. C. T.; Vrana, K.; Sharov, V.; Barrón, L.; Schöneich, C.; Quijano, C.; Alvarez, B.; others. Nitration and Inactivation of Tyrosine Hydroxylase by Peroxynitrite. *J. Biol. Chem.* **2001**, *276* (49), 46017–46023.
(33) Kobayashi, M.; Yasukawa, H.; Arikawa, T.; Deguchi, Y.; Mizushima, N.; Sakurai, M.; Onishi, S.; Tagawa, R.; Sudo, Y.; Okita, N.; others. Trehalose Induces SQSTM1/P62 Expression and Enhances Lysosomal Activity and Antioxidative Capacity in Adipocytes. *FEBS Open Bio* **2021**, *11* (1), 185–194.
(34) Bardag-Gorce, F.; Francis, T.; Nan, L.; Li, J.; Lue, Y. H.; French, B. A.; French, S. W. Modifications in P62 Occur Due to Proteasome Inhibition in Alcoholic Liver Disease. *Life Sci.* **2005**, *77* (20), 2594–2602.
(35) Li, C.; Wang, X.; Li, X.; Qiu, K.; Jiao, F.; Liu, Y.; Kong, Q.; Liu, Y.; Wu, Y. Proteasome Inhibition Activates Autophagy-Lysosome Pathway Associated with TFEB Dephosphorylation and Nuclear Translocation. *Front. cell Dev. Biol.* **2019**, *7*, 170.
(36) Abokyi, S.; To, C.; Chan, H. H.; Tse, D. Y.; others. Autophagy Upregulation by the TFEB Inducer Trehalose Protects against Oxidative Damage and Cell Death Associated with NRF2 Inhibition in Human RPE Cells. *Oxid. Med. Cell. Longev.* **2020**, *2020*.
(37) Kabeya, Y.; Mizushima, N.; Ueno, T.; Yamamoto, A.; Kirisako, T.; Noda, T.; Kominami, E.; Ohsumi, Y.; Yoshimori, T. LC3, a Mammalian Homologue of Yeast Apg8p, Is Localized in Autophagosome Membranes after Processing. *EMBO J.* **2000**, *19* (21), 5720–5728.
(38) Sarkar, S.; Davies, J. E.; Huang, Z.; Tunnacliffe, A.; Rubinsztein, D. C. Trehalose, a Novel MTOR-Independent Autophagy Enhancer, Accelerates the Clearance of Mutant Huntingtin and α-Synuclein. *J. Biol. Chem.* **2007**, *282* (8), 5641–5652.
(39) Zhang, J.; Yi, M.; Zha, L.; Chen, S.; Li, Z.; Li, C.; Gong, M.; Deng, H.; Chu, X.; Chen, J.; others. Sodium Butyrate Induces Endoplasmic Reticulum Stress and Autophagy in Colorectal Cells: Implications for Apoptosis. *PLoS One* **2016**, *11* (1), e0147218.

(40) DeBosch, B. J.; Heitmeier, M. R.; Mayer, A. L.; Higgins, C. B.; Crowley, J. R.; Kraft, T. E.; Chi, M.; Newberry, E. P.; Chen, Z.; Finck, B. N.; others. Trehalose Inhibits Solute Carrier 2A (SLC2A) Proteins to Induce Autophagy and Prevent Hepatic Steatosis. *Sci. Signal.* **2016**, *9* (416), ra21--ra21.

(41) Minutoli, L.; Altavilla, D.; Bitto, A.; Polito, F.; Bellocco, E.; Laganà, G.; Fiumara, T.; Magazù, S.; Migliardo, F.; Venuti, F. S.; others. Trehalose: A Biophysics Approach to Modulate the Inflammatory Response during Endotoxic Shock. *Eur. J. Pharmacol.* **2008**, *589* (1–3), 272–280.

(42) Pagliassotti, M. J.; Estrada, A. L.; Hudson, W. M.; Wei, Y.; Wang, D.; Seals, D. R.; Zigler, M. L.; LaRocca, T. J. Trehalose Supplementation Reduces Hepatic Endoplasmic Reticulum Stress and Inflammatory Signaling in Old Mice. *J. Nutr. Biochem.* **2017**, *45*, 15–23.

(43) Aoki, N.; Furukawa, S.; Sato, K.; Kurokawa, Y.; Kanda, S.; Takahashi, Y.; Mitsuzumi, H.; Itabashi, H. Supplementation of the Diet of Dairy Cows with Trehalose Results in Milk with Low Lipid Peroxide and High Antioxidant Content. *J. Dairy Sci.* **2010**, *93* (9), 4189–4195.

(44) Aoki, N.; Sato, K.; Kanda, S.; Mukai, K.; Obara, Y.; Itabashi, H. Time Course of Changes in Antioxidant Activity of Milk from Dairy Cows Fed a Trehalose-Supplemented Diet. *Anim. Sci. J.* **2013**, *84* (1), 42–47.

(45) Chen, G.; Ran, X.; Li, B.; Li, Y.; He, D.; Huang, B.; Fu, S.; Liu, J.; Wang, W. Sodium Butyrate Inhibits Inflammation and Maintains Epithelium Barrier Integrity in a TNBS-Induced Inflammatory Bowel Disease Mice Model. *EBioMedicine* **2018**, *30*, 317–325.

(46) Qiao, C.-M.; Sun, M.-F.; Jia, X.-B.; Li, Y.; Zhang, B.-P.; Zhao, L.-P.; Shi, Y.; Zhou, Z.-L.; Zhu, Y.-L.; Cui, C.; others. Sodium Butyrate Exacerbates Parkinson's Disease by Aggravating Neuroinflammation and Colonic Inflammation in MPTP-Induced Mice Model. *Neurochem. Res.* **2020**, *45* (9), 2128–2142.

(47) Sampson, T. R.; Debelius, J. W.; Thron, T.; Janssen, S.; Shastri, G. G.; Ilhan, Z. E.; Challis, C.; Schretter, C. E.; Rocha, S.; Gradinaru, V.; others. Gut Microbiota Regulate Motor Deficits and Neuroinflammation in a Model of Parkinson's Disease. *Cell* **2016**, *167* (6), 1469–1480.

(48) Tanaka, M.; Machida, Y.; Niu, S.; Ikeda, T.; Jana, N. R.; Doi, H.; Kurosawa, M.; Nekooki, M.; Nukina, N. Trehalose Alleviates Polyglutamine-Mediated Pathology in a Mouse Model of Huntington Disease. *Nat. Med.* **2004**, *10* (2), 148–154.

(49) Castillo, K.; Nassif, M.; Valenzuela, V.; Rojas, F.; Matus, S.; Mercado, G.; Court, F. A.; van Zundert, B.; Hetz, C. Trehalose Delays the Progression of Amyotrophic Lateral Sclerosis by Enhancing Autophagy in Motoneurons. *Autophagy* **2013**, *9* (9), 1308–1320.

(50) Lee, H.-J.; Yoon, Y.-S.; Lee, S.-J. Mechanism of Neuroprotection by Trehalose: Controversy Surrounding Autophagy Induction. *Cell death \& Dis.* **2018**, *9* (7), 1–12.

(51) Kam, T.-I.; Mao, X.; Park, H.; Chou, S.-C.; Karuppagounder, S. S.; Umanah, G. E.; Yun, S. P.; Brahmachari, S.; Panicker, N.; Chen, R.; others. Poly (ADP-Ribose) Drives Pathologic α-Synuclein Neurodegeneration in Parkinson's Disease. *Science (80-.).* **2018**, *362* (6414).

(52) Sharma, S.; Deshmukh, R. Vinpocetine Attenuates MPTP-Induced Motor Deficit and Biochemical Abnormalities in Wistar Rats. *Neuroscience* **2015**, *286*, 393–403.

(53) Crusio, W. E. The Genetics of Exploratory Behavior. In *Behavioral Genetics of the Mouse*; Crusio, Wim E; Sluyter, Frans; Gerlai, Robert T; Pietropaolo, S., Ed.; Cambridge University Press: Cambridge, United Kingdom, 2013; pp 148–154. https://doi.org/10.1017/cbo9781139541022.

(54) Crusio, Wim E; Sluyter, Frans; Gerlai, R. T. Ethogram of the Mouse. In *Behavioral Genetics of the Mouse*; Wim, E Crusio; Frans, Sluyter; Gerlai, Robert T; Pietropaolo,

S., Ed.; Cambridge University Press: Cambridge, United Kingdom, 2013; pp 17–22.
(55) Luong, T. N.; Carlisle, H. J.; Southwell, A.; Patterson, P. H. Assessment of Motor Balance and Coordination in Mice Using the Balance Beam. *JoVE (Journal Vis. Exp.* **2011**, No. 49, e2376.
(56) Quillfeldt, J. A. Behavioral Methods to Study Learning and Memory in Rats. In *Rodent Model as Tools in Ethical Biomedical Research*; Springer, 2016; pp 271–311.
(57) Antunes, M.; Biala, G. The Novel Object Recognition Memory: Neurobiology, Test Procedure, and Its Modifications. *Cogn. Process.* **2012**, *13* (2), 93–110.
(58) Lowry, O. H.; Rosebrough, N. J.; Farr, A. L.; Randall, R. J.; others. Protein Measurement with the Folin Phenol Reagent. *J. Biol. Chem.* **1951**, *193*, 265–275.
(59) Sarathlal, K. C.; Kakoty, V.; Marathe, S.; Chitkara, D.; Taliyan, R. Exploring the Neuroprotective Potential of Rosiglitazone Embedded Nanocarrier System on Streptozotocin Induced Mice Model of Alzheimer's Disease. *Neurotox. Res.* **2020**, 1–16.

Supporting Information

Neuroprotective Effect of Trehalose and Sodium Butyrate on Preformed Fibrillar Form of Alpha-Synuclein Induced Rat Model of Parkinson Disease

Violina Kakoty[1], Sarathlal K C[1], Sunil Kumar Dubey[1], Chih-Hao Yang[2], Rajeev Taliyan[1*]

[1]Neuropsychopharmacology Division, Department of Pharmacy, Birla Institute of Technology and Science-Pilani, Pilani Campus-333031, Rajasthan, India

[2]Department of Pharmacology, Taipei Medical University, Taipei-110, Taiwan

Corresponding author
Prof. Rajeev Taliyan, PhD
Associate professor
Department of Pharmacy,
Birla Institute of Technology and Science, Pilani-333031, Rajasthan, India
Mob: (+91) 8769196560, E-mail: taliyanraja@gmail.com

1. Validation of intra-striatal coordinates

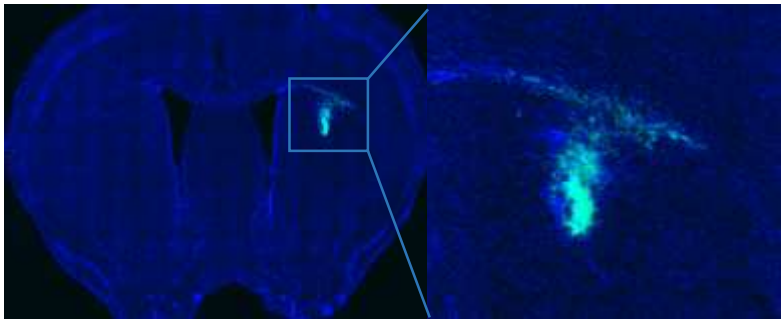

Supplementary Fig. 1: Striatum section of brain showing the presence of green fluorescent protein

2. **Sedimentation assay for confirmation of fibril, active PFF, Coomasie staining**

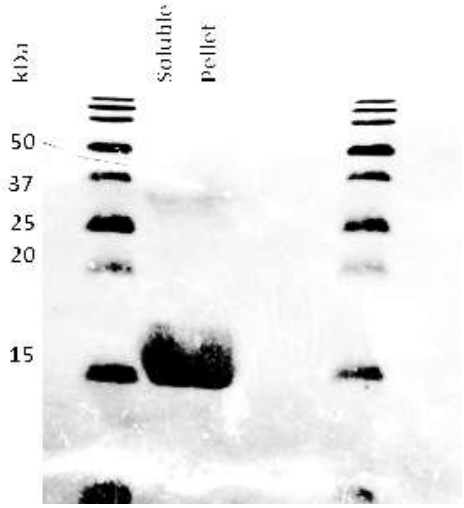

Supplementary Fig. 2: Confirmation assay for fibril, active PFF

3. **Effect of Tre and SB on NOR and NOL test**

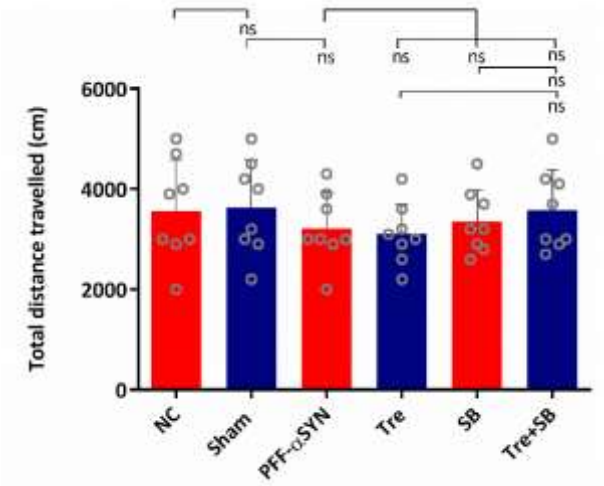

Supplementary Fig. 3a: The results were found to be statistically insignificant for all the groups during habituation phase i.e. stage 1, F (5,42) = 0.5865, P = 0.7102, ns: non-significant, NC: normal control.

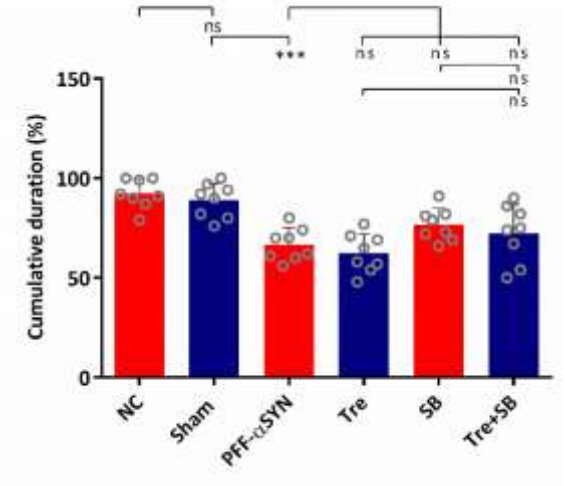

Supplementary Fig. 3b: Effect of tre and SB during training phase (stage 2): ***P≤0.001 (Sham vs PFF α-syn); ns (PFF α-syn vs Tre); ns P≤0.01 (PFF α-syn vs SB); ns (PFF α-syn vs Tre+SB); ns (tre+SB vs tre); ns (tre+SB vs SB), F (5,42) = 12.17, P < 0.0001, ns: non-significant, NC: normal control.

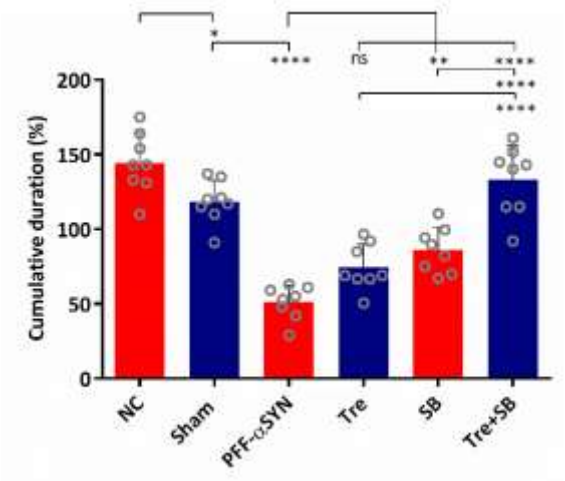

Supplementary Fig. 3c: Effect of tre and SB on novel object recognition test (stage 3): Values represents Mean ± SD, ****P≤0.0001 (Sham vs PFF α-syn); ns (PFF α-syn vs Tre); ****P≤0.0001 (PFF α-syn vs SB); ****P≤0.0001 (PFF α-syn vs Tre+SB); ****P≤0.0001 (tre+SB vs tre); ****P≤0.0001 (tre+SB vs SB), F (5,42) = 35.92, P < 0.0001, ns: non-significant, NC: normal control.

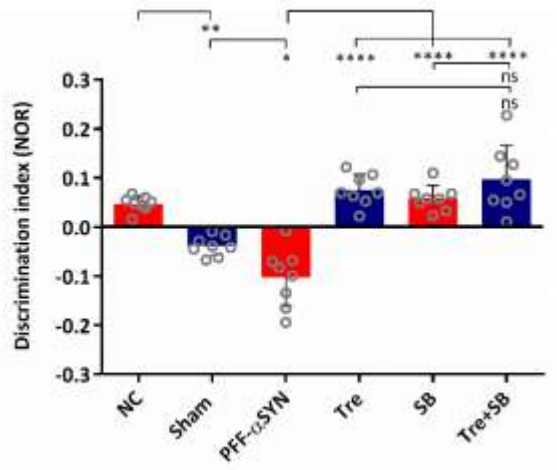

Supplementary Fig. 3d: Effect of Tre and SB on discrimination index for novel object recognition test: Values represents Mean ± SD, *P≤0.05, (Sham vs PFF α-syn); ****P≤0.0001 (PFF α-syn vs Tre); ****P≤0.0001 (PFF α-syn vs SB); ****P≤0.0001 (PFF α-syn vs Tre+SB); ns (tre+SB vs tre); ns (tre+SB vs SB), F (5,42) = 27.01, P < 0.0001, ns: non-significant, NC: normal control.

.

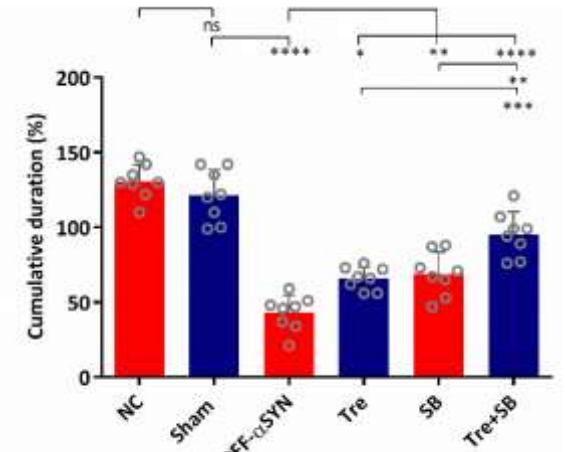

Supplementary Fig. 3e: Effect of tre and SB on novel object location test (stage 4): Values represents Mean ± SD, ****P≤0.0001, (Sham vs PFF α-syn); ns (PFF α-syn vs Tre); **P≤0.01 (PFF α-syn vs SB); ****P≤0.0001 (PFF α-syn vs Tre+SB); ***P≤0.001 (tre+SB vs tre); **P≤0.01 (tre+SB vs SB), F (5,42) = 52.81, P < 0.0001, ns: non-significant, NC: normal contro

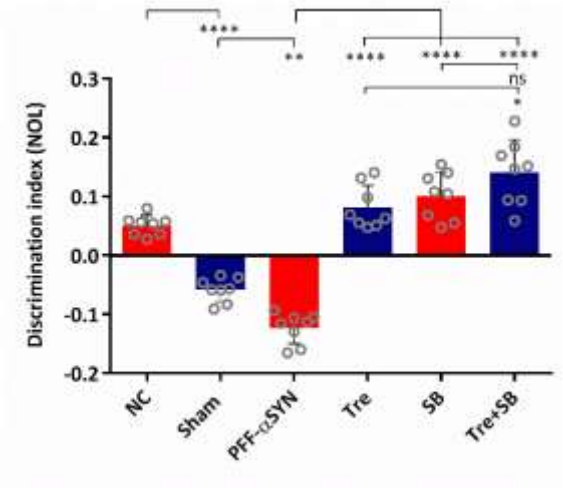

Supplementary Fig. 3f: Effect of tre and SB on discrimination index for novel object location test: Values represents Mean ± SD, **P≤0.01, (Sham vs PFF α-syn); ****P≤0.0001 (PFF α-syn vs Tre); ****P≤0.0001 (PFF α-syn vs SB); ****P≤0.0001 (PFF α-syn vs Tre+SB); *P≤0.05 (tre+SB vs tre); ns (tre+SB vs SB), F (5,42) = 66.54, P < 0.0001, ns: non-significant, NC: normal control.

4. Histopathological analysis

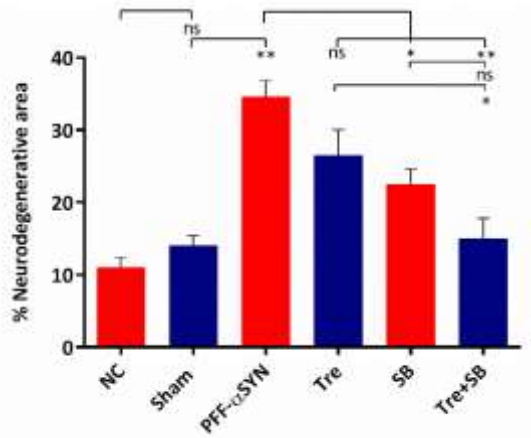

Supplementary Fig. 4: Quantified data for H & E analysis of the SN region of the brain: Analysis of the degenerative area using image J software revealed **P≤0.01 (Sham vs PFF α-

syn); ns (PFF α-syn vs Tre); $^{*}P \leq 0.05$ (PFF α-syn vs SB); $^{**}P \leq 0.01$ (PFF α-syn vs Tre+SB); $^{*}P \leq 0.05$ (tre+SB vs tre); ns (tre+SB vs SB), $F(5,6) = 28.28$, $P = 0.0004$, Values represented as Mean ± SD, ns: non-significant, NC: normal control.

Violina kakoty

Signature of the applicant